



# Catchment-scale stream network spatio-temporal models, applied to the freshwater stages of a diadromous fish species, longfin eel (*Anguilla dieffenbachii*)

Anthony R. Charsley<sup>a,\*</sup>, Arnaud Grüss<sup>a</sup>, James T. Thorson<sup>b</sup>, Merrill B. Rudd<sup>c</sup>, Shannan K. Crow<sup>d</sup>, Bruno David<sup>e</sup>, Erica K. Williams<sup>a</sup>, Simon D. Hoyle<sup>f</sup>

<sup>a</sup> National Institute of Water and Atmospheric Research, 301 Evans Bay Parade, Greta Point, Wellington 6021, New Zealand

<sup>b</sup> Habitat and Ecological Processes Research Program, Alaska Fisheries Science Center, National Marine Fisheries Service, NOAA, 7600 Sand Point Way N.E., Seattle, WA 98115, USA

<sup>c</sup> Scaleability LLC, 3718 34th Avenue SW, Seattle, WA 98126, USA

<sup>d</sup> National Institute of Water and Atmospheric Research, 10 Kyle Street, Riccarton, Christchurch 8011, New Zealand

<sup>e</sup> Waikato Regional Council, 160 Ward Street, Private Bag 3038, Waikato Mail Centre, Hamilton 3204, New Zealand

<sup>f</sup> National Institute of Water and Atmospheric Research, 217 Akersten St., Port Nelson, Nelson 7010, New Zealand



## ARTICLE INFO

Handled by Jie Cao

**Keywords:**

Spatio-temporal stream network models  
VAST modelling platform  
Ornstein-Uhlenbeck process  
Diadromous species  
Longfin eel

## ABSTRACT

Spatio-temporal modelling frameworks are important tools for evaluating changes in the population structure of freshwater species, to inform population assessments. However, in the stream networks occupied by freshwater species, two data points in space are more related by physical connectivity than by straight-line, Euclidian distance. Therefore, there is a need for spatio-temporal modelling frameworks that represent the relatedness of points based on physical connectivity. We developed such a modelling framework, known as the ‘VAST stream network modelling framework’, using the widely-employed vector autoregressive spatio-temporal modelling platform VAST and the Ornstein-Uhlenbeck process for spatial variance. Here, we demonstrate the VAST stream network spatio-temporal modelling platform with two applications to the freshwater stages of a diadromous fish species, the endemic New Zealand longfin eel (*Anguilla dieffenbachii*), and a simulation experiment. The first real-world application considers a single category (longfin eel) and models its probability of encounter in the Waitaki catchment, while the second distinguishes between two categories (smaller and larger longfin eels) and models their numerical densities in the greater Waikato region. These two applications demonstrate how stream network spatio-temporal models can usefully inform freshwater resource managers, providing insights into changes in fish encounter probability and density for different fish length classes and estimates of effective river length occupied. The simulation experiment uses the Waikato model as an operating model to evaluate alternative sampling scenarios for accuracy, precision and coverage, to advise on data requirements. A yearly sample size of 30 sites over a 20-year time series had the greatest precision and accuracy in trend estimates among all scenarios investigated. We also found that, for the scenario with declining female spawning biomass, increasing the yearly sample size from 15 sites to 30 sites in a 9-year time series increased the precision and resulted in unbiased estimates. There is a need to optimise sampling schemes for the freshwater stages of diadromous species, including longfin eel, and we, therefore, recommend further simulation experiments to explore scenarios of population trends, habitat features and sampling approaches.

## 1. Introduction

Globally, many diadromous fish populations (i.e., fish species that

must migrate between freshwater and marine habitats to complete their lifecycle) are declining, including numerous eel populations (e.g., International Council for the Exploration of the Sea (ICES). (2018); Jacoby

\* Corresponding author.

E-mail addresses: [Anthony.Charsley@niwa.co.nz](mailto:Anthony.Charsley@niwa.co.nz) (A.R. Charsley), [Arnaud.Gruss@niwa.co.nz](mailto:Arnaud.Gruss@niwa.co.nz) (A. Grüss), [James.Thorson@noaa.gov](mailto:James.Thorson@noaa.gov) (J.T. Thorson), [merrillrudd@gmail.com](mailto:merrillrudd@gmail.com) (M.B. Rudd), [Shannan.Crow@niwa.co.nz](mailto:Shannan.Crow@niwa.co.nz) (S.K. Crow), [bruno1david@gmail.com](mailto:bruno1david@gmail.com) (B. David), [Erica.Williams@niwa.co.nz](mailto:Erica.Williams@niwa.co.nz) (E.K. Williams), [Simon.Hoyle@niwa.co.nz](mailto:Simon.Hoyle@niwa.co.nz) (S.D. Hoyle).

et al., 2017; Ohlberger et al., 2016; Tanaka, 2014). In New Zealand freshwater ecosystems, longfin eel (*Anguilla dieffenbachii*) has shown a decreasing trend over the last 40 years and is currently listed as "endangered" (Pike et al., 2019). Longfin eel are a catadromous species, i.e., spends most of its life in freshwater habitats and emigrates to marine habitats to spawn. Longfin eel are endemic to New Zealand and are found throughout the country, preferring flowing waters in areas that are further inland than New Zealand's other common eel species, the shortfin eel (*Anguilla australis*) (Jellyman et al., 2003; McDowall and Taylor, 2000). The precise locations where longfin eel spawn are unknown, although magnetic orientation has been hypothesized during spawning (Durif et al., 2022). Longfin eel larvae spend nine to ten months in the marine environment, after which "glass eels" (55–70 mm) recruit into New Zealand freshwater habitats (Jellyman et al., 1999, 2002).

During their freshwater life stage, longfin eel population dynamics are impacted by natural and anthropogenic processes at both fine and catchment scales. For example, depth, flow velocity and cover affect the densities and length distributions of longfin eel at a site level (Booker and Graynoth, 2013). Anthropogenic factors affecting longfin eel include, among other things, fishing pressure, pollution, wetland drainage, removal of instream structural cover, and land development (Graynoth et al., 2008; Jellyman, 1997). In addition, longfin eel upstream and downstream passage in some New Zealand catchments is compromised by hydro-electric dams and weirs, which substantially reduce the availability of habitat for longfin eel to grow and reach spawning maturity (Graynoth et al., 2008; Hoyle, 2016).

The longfin eel is a cultural and ecological keystone species that supports important commercial, recreational, and customary fisheries. Therefore, it is paramount to assess the impacts of natural and anthropogenic activities to enable effective management. In particular, longfin eel are included in New Zealand's Quota Management System, but the current stock size of longfin eel and the fishing levels resulting in longfin eel maximum sustainable yield are unknown (Hoyle, 2016). Therefore, there is a critical need to develop methods for estimating spatio-temporal changes in longfin eel populations in New Zealand catchments, in relation to natural and anthropogenic drivers (Haro et al., 2015). The indices of abundance and fish length/age composition estimates generated by these models will represent key information for determining the status of longfin eel stocks.

Species distribution models (SDMs) using fishery-independent data, collected at the local and/or catchment level, are appropriate tools for estimating spatio-temporal changes in longfin eel populations in the freshwater environment. First, longfin eel are distributed fractally during their freshwater phase, extending from the sea, up rivers, and into lakes and countless small streams and ditches, with low movement rates and mixing between the multiple habitat areas (Hoyle, 2016). After glass eels recruit to individual catchments, there may be effectively no subsequent mixing between longfin eels in different catchments, or in different parts of the same catchment, until the mature eels emigrate out to sea and spawn many years later. As a result of this limited mixing, longfin eel population dynamics are strongly habitat-dependent and show very diverse growth rates (Jellyman, 1997), sex ratios (Davey and Jellyman, 2005; Geffroy and Bardouillet, 2016), and length and age compositions across New Zealand (Glova and Jellyman, 2000; Glova et al., 2001). Given the spatial variation in population dynamics, SDMs that incorporate the effects of natural and/or anthropogenic drivers at the local or catchment level appear most appropriate. Moreover, a proportion of the New Zealand longfin eel population and the majority of female spawning biomass inhabits unfished freshwater habitats, thereby providing a substantial fraction of the spawning biomass emigrating to marine habitats each year (Graynoth and Booker, 2009; Graynoth et al., 2008; Hoyle, 2016). Thus, SDMs relying solely on fishery-dependent data cannot provide reliable indices of abundance and length/age composition estimates for the entire population because of the substantial differences between fished and unfished substocks.

These differences among substocks are largely due to variation in demographic parameters and low mixing between freshwater habitat areas. Therefore, to accurately estimate spatio-temporal changes in eel populations in the New Zealand freshwater environment, it is more appropriate to fit SDMs for longfin eel with fishery-independent data (Hoyle, 2016).

Over the past 15–20 years, SDMs have been fitted to fishery-independent monitoring data to estimate longfin eel abundance or biomass in specific catchments or locations in New Zealand, in relation to environmental variables (Graynoth and Booker, 2009; Graynoth et al., 2008; Graynoth and Niven, 2004). These different SDMs have advanced our knowledge of the potential environmental influences on longfin eel density, abundance and biomass, and our understanding of the possible longfin eel biomass levels in fished and unfished areas. For example, Graynoth et al. (2008) fitted generalized additive models (GAMs) to fishery-independent biomass-density data for 212 rivers and streams located in various catchments throughout New Zealand. Longfin eel biomass-density was found to be largely influenced by the stream gradient and mean annual low flow of the study reach. Additionally, current longfin eel biomass and the biomass of longfin eel before the initiation of commercial fishing was estimated. While SDMs such as GAMs (Graynoth and Booker, 2009; Graynoth et al., 2008) provide insights into the environmental drivers of longfin eel populations and their potential biomass levels, they were not specified to account for spatio-temporal structure (spatio-temporal autocorrelation) in the data. Such spatial, temporal, and spatio-temporal random effects would be able to capture unknown or unspecified processes driving the variability in longfin eel populations. Therefore, it is generally recommended that spatial terms are included in SDMs by default (Thorson, 2019a).

Spatio-temporal modelling platforms such as the vector autoregressive spatio-temporal (VAST) modelling platform (Thorson, 2019a; Thorson and Barnett, 2017) were identified as very relevant tools for longfin eel populations. VAST is a recently-developed tool that accounts for both spatial (stable over time) and spatio-temporal (changing over time) variation at a very fine scale, and can include environmental and catchability covariates (Thorson, 2019a; Thorson and Barnett, 2017). VAST has been increasingly employed to support assessments of stocks (e.g., Cao et al., 2017; Grüss et al., 2019b; Thorson and Haltuch, 2018; Thorson et al., 2015), habitats (e.g., Grüss et al., 2019a; Grüss et al., 2020b; Grüss and Thorson, 2019; Kai et al., 2017), ecosystems (e.g., Duffy-Anderson et al., 2019; Thorson et al., 2019; Thorson and Barnett, 2017) and climate-vulnerability (e.g., Thorson, 2019b). The key tenet of the VAST spatio-temporal modelling platform is that two points in space are more strongly correlated if they are neighbours (i.e., close in space). To date, their degree of correlation has been based on a linear transformation of their Euclidian (or spherical) distance (Thorson, 2019a).

In stream networks, two points in space are related by their proximity within the stream network rather than by Euclidian distance which in many cases will include dry land between streams. Spatial stream network models (SSN models; e.g., Isaak et al., 2014; Isaak et al., 2016; Peterson et al., 2013; Ver Hoef et al., 2014; Ver Hoef et al., 2019) represent spatial structure based on connectivity along a stream network, but typically do not include a temporal correlation component (i.e., individual years are estimated independently). However, many relationships within stream networks are maintained from one year to the next, so estimates across multiple years can be substantially more reliable and with less uncertainty. Therefore, there is a need to develop VAST spatio-temporal models that build upon SSN models by relating points in space based on physical connectivity within the river network, while also including a temporal correlation component.

In this paper, we present and apply a new implementation of the VAST spatio-temporal modelling platform for longfin eel. This new implementation specifies an Ornstein-Uhlenbeck process to represent the relatedness of points in space within a stream network. This paper extends the implementation in Hocking et al. (2018) and is the first publication to demonstrate the "VAST stream network modelling

framework". We present three applications of the VAST stream network modelling framework (Fig. 1): (1) a longfin eel probability of encounter model for the Waitaki catchment; (2) a density model for the greater Waikato region that considers eel length classes; and (3) a simulation experiment to determine data requirements for estimating trends in female spawning biomass in the greater Waikato region with a certain level of accuracy and precision and a good representation of uncertainty (well-performing confidence intervals). The three applications use fishery-independent data to accurately estimate spatio-temporal changes for longfin eel in the New Zealand freshwater environment (i.e., whether fished or unfished; Hoyle, 2016). This spatio-temporal stream network VAST model has also been recently applied to the freshwater stages of an anadromous fish population (i.e., a fish population that spends most of its life in marine habitats and must migrate to freshwater to spawn), the coho salmon (*Oncorhynchus kisutch*) population of the Siletz River watershed in Oregon, USA (Rudd, pers. comm.). Together, the three applications reported here and the application of Rudd (pers. comm.) represent a solid foundation for future spatio-temporal modelling studies of riverine freshwater species using the VAST stream network modelling framework.

## 2. Methods

We developed a modelling framework based on the VAST spatio-temporal modelling platform and the Ornstein-Uhlenbeck (OU) algorithm to represent the relatedness of points in space within a stream network. We refer to this framework as the "VAST stream network modelling framework". In the following, we describe the VAST

modelling platform and the VAST stream network modelling framework. Then, we describe the longfin eel and covariate data compiled and used for the present study. Finally, we present three applications of the framework to longfin eel.

### 2.1. The VAST modelling platform

VAST is a flexible modelling platform designed to answer a wide range of questions in fisheries stock, habitat, climate, and ecosystem assessments (see Table 1 in Thorson, 2019a). Models are implemented in the R statistical environment (R Core Team, 2020) using the "VAST" software package (<http://www.github.com/james-thorson/VAST>) (Thorson, 2019a; Thorson and Barnett, 2017). Generally, the analyst uses VAST models to generate population estimates (e.g., density) and/or derive population metrics (e.g., effective area occupied) over a user-specified spatial domain. As such, building a representative spatial domain is an important aspect of the modelling process.

VAST is flexible enough to model univariate or multivariate responses through its 'category' feature. Where VAST uses a 'category' as a univariate response or multiple 'categories' as multivariate responses. Categories are user-specified and can be, for example, single or multiple species, ages, lengths, or life stages. When multiple species are used, the model becomes a joint-species distribution model (JSDM) (Thorson and Barnett, 2017).

VAST can distinguish between covariate types and is able to account for unmeasured processes. Covariate types include habitat covariates which measure aspects of the habitat within the spatial domain (e.g., water temperature) and catchability covariates which describe

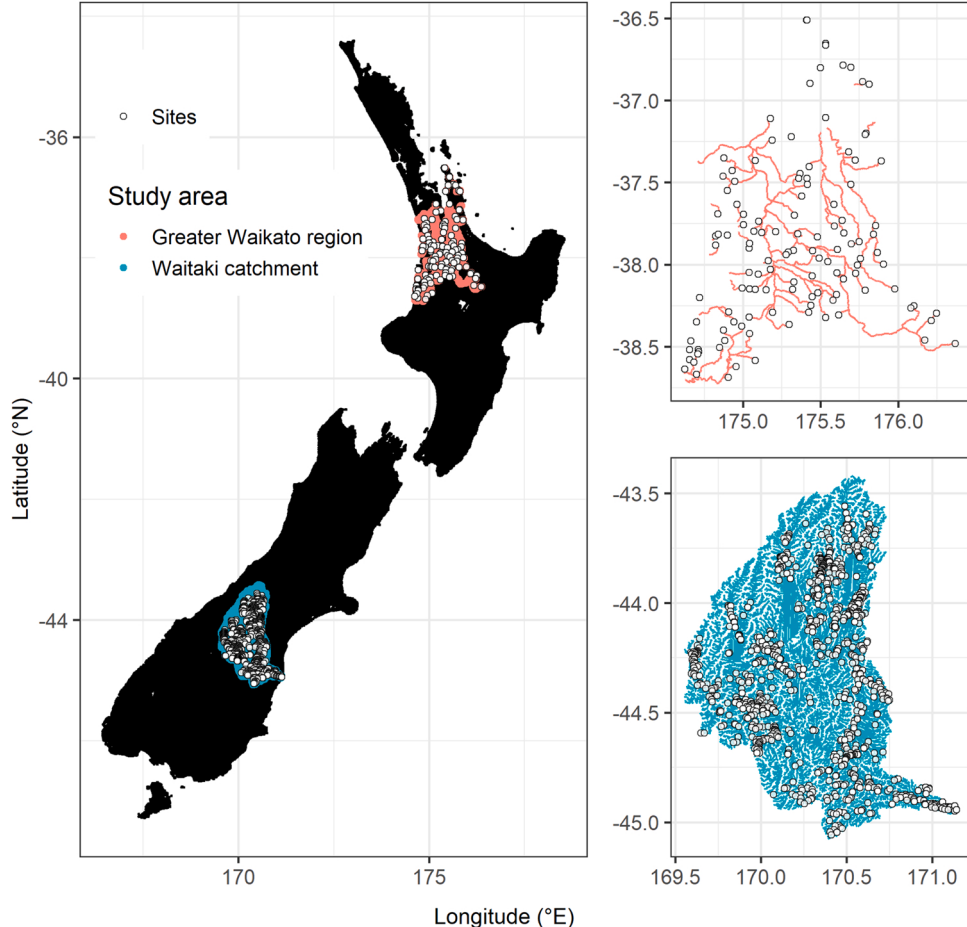


**Fig. 1.** The electric fishing sites (circles), across time, in the greater Waikato region (top-right) and the Waitaki catchment (bottom-right) study areas of New Zealand (left). The study areas were used in VAST as stream network spatial domains.

differences in the response variable of interest due to sampling features (e.g., fishing method). Where VAST models condition on habitat covariates to improve model predictions. Unmeasured processes are approximated through spatial and spatio-temporal random effects. VAST models use the measured habitat and catchability covariates along with the random effects for the unmeasured processes to derive population metrics (Thorson, 2019a).

VAST models can be fitted to different data types. Continuous response variables such as numerical density, biomass-density or biomass data are modelled using a delta (a.k.a. hurdle) approach involving two linear models whose predictions are combined to produce outputs of interest (e.g., distribution maps, indices of abundance) (Lo et al., 1992; Stefánsson, 1996; Thorson, 2018). Biomass-density is

model), the second component is ‘switched off’ (Grüss et al., 2017; Thorson, 2019c). In comparison, counts are modelled using a delta model for count data that combines the predictions of a zero-inflation probability model and a count-data intensity model (Thorson, 2019c; Thorson and Barnett, 2017).

The first linear predictor of a VAST model,  $p_1$ , is employed to estimate probability of encounter (when working with encounter/non-encounter or continuous data) or zero-inflation probability (when working with count data). For instance, when probability of encounter is modelled using a binomial distribution model, it is obtained via a logit transformation of  $p_1$ . The predictor  $p_1$  is expressed as a linear combination of temporal, spatial and spatio-temporal variation terms, habitat covariates, and catchability covariates:

$$\begin{aligned}
 p_1(i) = & \underbrace{\mu_{\beta 1}(c_i)}_{\text{Temporal variation}} + \underbrace{\sum_{f=1}^{n_{\beta 1}} L_{\beta 1}(c_i, f) \beta_1(t_i, f)}_{\text{Spatial variation}} + \underbrace{\sum_{f=1}^{n_{\omega 1}} L_{\omega 1}(c_i, f) \omega_1(s_i, f)}_{\text{Spatio-temporal variation}} + \\
 & \underbrace{\sum_{p=1}^{n_p} \gamma_1(c_i, t_i, p) X(s_i, t_i, p)}_{\text{Habitat covariates}} + \underbrace{\sum_{k=1}^{n_k} \lambda_1(k) Q(i, k)}_{\text{catchability covariates}}
 \end{aligned} \quad (1)$$

commonly used and can be modelled using a delta-Gamma model, where (1) a binomial model is fitted to encounters/non-encounters to generate estimates of probability of encounter and (2) a Gamma model is fitted to non-zero biomass catch rate to generate positive biomass-density estimates. When the analyst is interested only in the first component of the delta model (i.e., the probability of encounter

**Table 1**  
Description of the parameters used in the spatio-temporal stream network model. The subscripts here are for the first component of the delta model; parameter descriptions for the second component of the delta model are identical but with different subscripts (e.g.,  $p_2(i)$ ).

Parameter	Description
<i>Ornstein-Uhlenbeck process</i>	
$\omega(s)$	Degree of correlation between location $s$ and parent node $s_{parent}$
$\rho_s(s)$	Expected correlation between points on the stream network
$\sigma_s^2(s)$	Variance for location $s$ conditioned on the value for parent $s_{parent}$
$\theta_\epsilon$	Exponential rate of decorrelation between child and parent nodes
$\sigma_\epsilon^2$	Asymptotic variance from an Ornstein-Uhlenbeck process for two locations that are infinitely far apart
<i>Linear predictors</i>	
$p_1(i)$	Encounter probability for observation $i$
$\beta_1(c_i)$	Average time effect for the category associated with observation $i$ , $c_i$
$L_{\beta 1}(c_i)$	Loadings matrix that generates temporal covariation among categories
$\beta_1(t_i)$	Temporal variation for the time associated with observation $i$ , $t_i$
$L_{\omega 1}(c_i)$	Loadings matrix that generates spatial covariation among categories for observation $i$
$\omega_1(s_i)$	Spatial variation occurring at the location associated with observation $i$ (sites), $s_i$
$L_{\epsilon 1}(c_i)$	Loadings matrix that generates spatio-temporal covariation among categories
$\epsilon_1(s_i, t_i)$	Spatio-temporal variation at site $s_i$
$X(i, t_i, p)$	Three-dimensional array of $n_p$ measured density covariates that explain density for time $t_i$ and site $s_i$
$\gamma_1(c_i, t_i, p)$	Average effect of density covariate $X(i, t_i, p)$ for category $c_i$
$Q(i, k)$	Matrix of $n_k$ measured catchability covariates that explain catchability for observation $i$
$\lambda_1(k)$	Impact of catchability covariate $k$
<i>Temporal and spatio-temporal structure</i>	
$\rho_{\beta 1}$	Degree of first-order autocorrelation in temporal variation
$\sigma_{\beta 1}$	Standard deviation for normally distributed values on temporal smoother
$\rho_{\epsilon 1}$	Degree of first-order autocorrelation in spatio-temporal variation
$t_{min}$	Index for the first modelled year

where  $p_1(i)$  is the value of the first linear predictor for observation  $i$ ; and the temporal, spatial and spatio-temporal variation terms are described in detail below (see Subsections 2.1.1 to 2.1.3). The terms in Eq. (1) are a function of observation  $i$ , category  $c$ , time  $t$ , factor  $f$ , location  $s$  (referred to as ‘sites’ throughout this paper when there is an observation associated with the location, i.e.,  $s_i$ ), habitat covariate  $p$ , or catchability covariate  $k$ . When a single category  $c$ , is used, the model has a univariate response but when multiple categories are used, the model has a multivariate response. Factors  $f$ , are used for spatial factor analysis, where usually a temporal, spatial, and spatio-temporal factor is set for each category in a model or are ignored in a single category model (Thorson et al., 2015). Eq. (1) formulates  $p_1(i)$  assuming multiple categories. In the case of a single category,  $c$  can be ignored. Habitat covariates are variables that describe differences in the response variable of interest due to explicit habitat features. The  $X(s_i, t_i, p)$  term is an array of  $n_p$  habitat covariates measured at locations associated with observation  $i$ ,  $s_i$  (sites) and the time associated with observation  $i$ ,  $t_i$ . The  $\gamma_1(c_i, t_i, p)$  term is the estimated effect of habitat covariate  $p$  for the category associated with observation  $i$ ,  $c_i$ , at time  $t_i$ . The  $Q(i, k)$  is a matrix of  $n_k$  measured catchability covariates that explain variation for observation  $i$ , and  $\lambda_1(k)$  represents the estimated effect of catchability covariate  $k$ .

The second linear predictor of the spatio-temporal model,  $p_2$ , is used to estimate positive abundance-density or positive biomass-density (when working with continuous data) or count-data intensity (when working with count data). It is expressed as a linear combination of temporal, spatial and spatio-temporal variation terms, habitat covariates and catchability covariates, as in Eq. (1). See Table 1 for a description of the different modelling terms of the first and second linear models.

VAST version 3.7.0 was employed for all the case studies reported in the present paper. All the fixed effects of the spatio-temporal models are estimated by determining the parameter values resulting in maximum marginal log-likelihood. The marginal log-likelihood is calculated via an approximation of the integral across all random effects using the Laplace approximation implemented by R package “TMB” (Kristensen et al., 2015). TMB (Template Model Builder) relies on automatic differentiation to compute in an efficient manner the matrix of second derivatives (which is used by the Laplace approximation) and the Laplace approximation gradient (which is used when the fixed effects are maximised).

All random effects are estimated by TMB by maximizing the marginal log-likelihood given the maximum likelihood estimates of the fixed effects. VAST relies on the generalized delta method implemented in TMB to compute the standard errors of all fixed and random effects and of the derived quantities (Kass and Steffey, 1989). Moreover, a bias-correction estimator (Thorson and Kristensen, 2016) is used to correct for “retransformation bias” when any derived quantity involving a non-linear transformation of the random effects is predicted.

To evaluate the fitted spatio-temporal models we compared multiple competing models. For each study, we built multiple models with different settings (e.g., fixed versus random temporal effects), structure (e.g., with and without spatio-temporal effects) and habitat covariates. We assessed each model for convergence, examined residuals calculated using R package “DHARMA” (Hartig, 2020) and calculated the Akaike Information Criterion (AIC) (Burnham and Anderson, 2002). Converged models had gradients of the marginal log-likelihood less than 0.0001 for all fixed effects, and positive definite Hessian matrices of secondary derivatives of the negative-likelihood. To evaluate the models, we used DHARMA to simulate residuals standardised between 0 and 1 (Hartig, 2020). Specifically, it simulates data from the fitted model and calculates their empirical density function. Residuals are the value of the calculated empirical density function at the value of each of the observed values. A residual of 0 indicates that all simulated values are greater than the observed value, while a residual of 0.5 indicates that half of the simulated values are greater than the observed value. Hence, models that fit well show an even spread of residuals between zero and one (Hartig, 2020). From the competing models that converged and fitted well, the model with the lowest AIC was selected.

### 2.1.1. Spatial variation

Because VAST builds upon factor analysis approaches (Thorson et al., 2015) to work with data for multiple categories (Thorson and Barnett, 2017), spatial variation (i.e., spatial structure that is constant over time) is expressed as the summation of a loadings matrix ( $L_{\omega 1}(c_i, f)$  or  $L_{\omega 2}(c_i, f)$ ) and the predicted spatial variation ( $\omega_1(s_i, f)$  or  $\omega_2(s_i, f)$ ), where the user can specify the number of factors (e.g.,  $n_{\omega 1}$  for the number of spatial factors in the 1st linear predictor) between 1 and the number of categories modelled. The loadings matrix expresses the estimated degree of association between each modelled category and each factor. It becomes a scalar when only one category is modelled.

Spatial variation is estimated as a random effect at each of  $n_s$  knots (locations within a grid or mesh spatial domain) or nodes (locations within a stream network spatial domain) using Gaussian random fields. For example, spatial variation in the first linear predictor is estimated as:

$$\omega_1(f) \sim MVN(\mathbf{0}, Q_1^{-1}) \quad (2)$$

where the vector  $\omega_1(f)$  of length  $n_s$  is formed by sub-setting  $\omega_1(s, f)$  for factor  $f$ ;  $MVN$  is the multivariate distribution; and  $Q_1^{-1}$  is the inverse-precision matrix defining the correlation between knots or each connected node. Note that the precision matrix for the second linear predictor,  $Q_2$ , is estimated independently of the precision matrix for the first linear predictor  $Q_1$ .

### 2.1.2. Spatio-temporal variation

Spatio-temporal variation (i.e., spatial structure that varies among years) is expressed as the summation of a loadings matrix ( $L_{\epsilon 1}(c_i, f)$  or  $L_{\epsilon 2}(c_i, f)$ ; which becomes a scalar when only one category is modelled) and the predicted spatio-temporal variation ( $\epsilon_1(s_i, f, t_i)$  or  $\epsilon_2(s_i, f, t_i)$ ). As is the case for spatial variation, spatio-temporal variation in each year is estimated as a random effect at each of  $n_s$  knots or node using Gaussian random fields. By default, the VAST modelling platform specifies spatio-temporal variation as independent among years, i.e., employs Eq. (2) to model spatio-temporal variation for each individual year. However, there are instances where it is more relevant to model spatio-temporal variation as a first-order autocorrelation process (e.g., when running

projections into the future; Thorson, 2019b); in those instance, spatio-temporal variation in the first linear predictor is estimated as:

$$\epsilon_1(f, t) \sim \begin{cases} MVN(\mathbf{0}, Q_1^{-1}) & \text{if } t = t_{\min} \\ MVN(\rho_{\epsilon_1} \epsilon_1(f, t - 1), Q_1^{-1}) & \text{if } t > t_{\min} \end{cases} \quad (3)$$

Where  $t_{\min}$  is the first time in the time series; and  $\rho_{\epsilon_1}$  is first-order temporal autocorrelation. Spatio-temporal variation can be specified as a random walk process ( $\rho_{\epsilon_1} = 1$ ), an autoregressive process ( $\rho_{\epsilon_1}$  is estimated as a fixed effect), or an individual autoregressive process ( $\rho_{\epsilon_1}$  is estimated for each category) (Thorson, 2019c).

### 2.1.3. Temporal variation

Temporal variation in the first linear predictor is given by:

$$\mu_{\beta 1}(c_i) + \sum_{f=1}^{n_{\beta 1}} L_{\beta 1}(c_i, f) \beta_1(t_i, f) \quad (4)$$

where the intercept  $\mu_{\beta 1}(c_i)$  gives the average temporal effect for each category  $c_i$ ; the term  $\beta_1(t_i, f)$  gives temporal variation for time  $t_i$  and factor  $f$ ; and the loadings matrix  $L_{\beta 1}(c_i, f)$  expresses the estimated degree of association between each modelled category and each factor, and becomes a scalar when only one category is modelled. Temporal variation in the second linear model is expressed similarly.

By default, the VAST modelling platform estimates temporal variation terms  $\beta_1(c_i, t_i)$  and  $\beta_2(c_i, t_i)$  as fixed effects. However, there are instances where it is more relevant to model temporal variation as a first-order autocorrelation process (e.g., some years of the time series are missing data; Thorson, 2019c); in those instances, first-order autocorrelation is employed to estimate temporal variation in the first linear predictor as a random effect as follows:

$$\beta_1(t, f) \sim \begin{cases} Normal(0, 1) & \text{if } t = t_{\min} \\ Normal(\rho_{\beta 1} \beta_1(t - 1, f), 1) & \text{if } t > t_{\min} \end{cases} \quad (5)$$

The parameter  $\rho_{\beta 1}$  controls the first-order autocorrelation and can be treated as independent among years ( $\rho_{\beta 1} = 0$ ), a random walk across time ( $\rho_{\beta 1} = 1$ ) or autoregressive ( $\rho_{\beta 1}$  is estimated as a fixed effect). It is also possible to treat the intercept as constant. First-order autocorrelation in temporal variation in the second linear model is modelled similarly as shown in Eq. (5).

## 2.2. The VAST stream network modelling framework

Here we provide an overview of the VAST stream network spatio-temporal modelling framework, which is based on the VAST platform (Thorson, 2019a). We begin by describing model spatial domains and the Ornstein-Uhlenbeck process. We then discuss the newly developed effective river length occupied metric.

### 2.2.1. The model spatial domain

When specifying a spatial model using Euclidean or spherical distance, the stochastic partial differential equation method (Lindgren et al., 2011) is employed to approximate the likelihood of random effects. This involves constructing a triangulated mesh to represent the relatedness of points in space. However, this way of representing spatial relationships is not appropriate when modelling stream networks, where points in space are more related based on distance within the river network rather than Euclidian distance. For this reason, we developed a novel approach within VAST to define spatial relationships, where spatial correlation can run throughout dendritic networks of streams and rivers as opposed to Euclidean distance.

In VAST stream network models, locations within the stream network (nodes) are associated with geographic coordinates, “child” (upstream) nodes and “parent” (downstream) nodes, and distances between connecting nodes. Each node is given a unique child node identifier, as well as a parent node identifier corresponding to the child node directly downstream of itself. Parent identifiers are non-unique because

more than one child node can flow into each parent (i.e., more than one stream can join downstream parent nodes). The river segments located the furthest downstream (usually connecting to the sea) are identified and classified as "root" nodes (i.e., the root of the stream network). Root nodes have parent identifiers of zero and an infinite distance-between-nodes value. These settings distinguish root nodes from other nodes.

For the present study, VAST stream networks were constructed using the River Environment Classification (REC) database (Snelder and Biggs, 2002) (see Fig. 1, right column). The REC database consists of unique river segments across New Zealand with corresponding environmental, hydrological, and spatial metadata. A 30-m digital elevation model was used to produce segments of river across the country that were, on average, approximately 700 m long (Crow et al., 2014; Snelder and Biggs, 2002; Snelder et al., 2004). Each segment is identified by a unique "nzsegment" code.

### 2.2.2. Ornstein-Uhlenbeck process for spatial correlation

The VAST stream network model specifies an Ornstein-Uhlenbeck (OU) process to estimate spatial correlation in stream networks. Hocking et al. (2018) demonstrated the utility of an OU process in a generalizable hierarchical model which we adapt here for use in VAST. We define the acyclic graph of upstream "child" and downstream "parent", such that each location where streams join or where data are available is treated as a "node". Therefore, for  $n_s$  total nodes, there are  $n_s$  stream segments each with stream length  $|s - s_{parent}|$ . This structure defines one or more "tree(s)", and each tree is rooted, i.e., has a parent node that is ancestor to all other nodes in that tree. The rooted node is then treated as having variance equal to the stationary distribution of the OU process.

With the OU process, spatial variation  $\omega(s)$  is estimated in a stream network so that the child node is correlated with the parent node as a function of distance (Hocking et al., 2018):

$$\omega(s)|\omega(s_{parent}) \sim \text{Normal}(\rho_s(s) \times \omega(s_{parent}), \sigma_s^2(s)) \quad (6)$$

where  $\rho_s$  gives the expected spatial correlation between points in the stream network; and  $\sigma_s^2(s)$  is the variance for spatial correlation for location  $s$ , conditioned upon the value for parent node  $s_{parent}$ , which is given by:

$$\sigma_s^2(s) = \frac{\sigma_\tau^2}{2\theta_\tau} \left( 1 - e^{-2\theta_\tau |s - s_{parent}|} \right) \quad (7)$$

where  $\theta_\tau$  determines the exponential rate of decorrelations between child and parent nodes, where larger values represent faster decorrelation;  $|s - s_{parent}|$  represents the distance between location  $s$  and parent node  $s_{parent}$ ; and  $\sigma_\tau^2$  determines the asymptotic variance for two infinitely distant nodes in an OU process. The expected correlation between points in a stream network,  $\rho_s(s)$ , is given by:

$$\rho_s(s) = e^{-\theta_\tau |s - s_{parent}|} \quad (8)$$

### 2.2.3. Joint specification of the Ornstein-Uhlenbeck process

To allow efficient software implementations, we have developed a function to calculate the inverse correlation matrix resulting from the conditional distributions in this OU process. This matrix  $\mathbf{Q}_{stream}$  is then used in place of the precision matrix  $\mathbf{Q}_{spde}$  that is typically constructed within VAST, and its use requires no further changes in software within TMB.  $\mathbf{Q}_{stream}$  is calculated from the single decorrelation rate parameter  $\theta_\tau$  (with units  $distance^{-1}$ ), analogous to how  $\mathbf{Q}_{spde}$  is calculated from decorrelation rate parameter  $\kappa$ .

For each segment ending at child node  $s$  we include:

$$Q_{stream}(s, s_{parent}) = Q_{stream}(s_{parent}, s) = \frac{-e^{-\theta_\tau |s - s_{parent}|}}{1 - e^{-2\theta_\tau |s - s_{parent}|}} \quad (9)$$

which represents the conditional dependence of child nodes given parent nodes. We further specify diagonal elements:

$$Q_{stream}(s, s) = 1 + \sum_{s' \in S} \frac{e^{-2\theta_\tau |s - s'|}}{1 - e^{-2\theta_\tau |s - s'|}} \quad (10)$$

where  $s' \in S$  is the set of child and parent nodes that are adjacent to node  $s$  (i.e., that are connected by a segment).

This joint distribution illustrates several properties of the OU process:

1. Any node  $s$  that is not otherwise connected with the network (i.e., a hypothetical pond with no aboveground out or inflow) has  $Q_{stream}(s, s) = 1$  and  $Q_{stream}(s, s^*) = 0$  for all other locations;
2. The determinant  $\det(Q_{stream}) = 1$ , such that the process has a unit variance, where the variance of the estimated spatial process is estimated via parameters outside of  $Q_{stream}$ ;
3. Any locations  $s$  and  $s^*$  that are not adjacent (i.e., that are not connected by a segment) have  $Q_{stream}(s, s^*) = 0$ , indicating that they are conditionally independent;
4. Any two portions of the stream network that do not share a common ancestor (i.e., belonging to catchments) will have nodes that are independent from one another, such that  $Q_{stream}^{-1}(s, s^*) = 0$  for any pair of nodes from those separate catchments.

### 2.2.4. Estimation of the effective river length occupied

With spatio-temporal models implemented with VAST that relate points in space using Euclidian distances, the effective area occupied by the population of interest (Thorson et al., 2016) is calculated by dividing the estimated abundance (or estimated biomass) by the average numerical density per  $km^2$  (or average biomass-density per  $km^2$ ) (Han et al., 2021). Calculating changes in effective area occupied provides insights into patterns of expansion or contraction. With spatio-temporal stream network models that relate points in space based on physical connectivity, we estimate the effective river length occupied rather than the effective area occupied. The same calculation as the effective area occupied is performed but average numerical density is expressed in average number per river length rather than per  $km^2$ . The ratio of estimated abundance and average number per river length can then be converted to a percentage by dividing the metric by the total length of all rivers in the catchment and multiplying by 100. We present results as a percentage to allow comparisons between catchments. Note that, with a binomial spatio-temporal stream network model, the effective river length occupied is, instead, the ratio of the sum of estimated encounter probability across all river segments and the average encounter probability per river length. As before, this is converted to a percentage.

## 2.3. Longfin eel data used in the present paper

### 2.3.1. The New Zealand Freshwater Fish Database (NZFFD)

We employed data from the New Zealand Freshwater Fish Database (NZFFD), a large database with over 34,000 records of mostly encounter/non-encounter data for New Zealand freshwater fishes (Crow, 2018). NZFFD records begin in the 1960 s and continue to be updated, spanning all of New Zealand's river network (see Fig. A1). The data have been voluntarily contributed by many organisations using various fishing methods, but currently, most data come from the National Institute of Water and Atmospheric Research (NIWA), and most are sampled using electric fishing. The NZFFD records are geo-located with coordinates and a unique "nzsegment" identifier, which links NZFFD records to REC locations and, therefore, the VAST stream network modelling framework.

New Zealand freshwater fish sampling protocols were established to reduce uncertainty about the protocols followed (Joy et al., 2013). However, a "sampling organisation" catchability factor was incorporated into longfin eel models to account for any differences in catchability between sampling organisations (e.g., due to different target species when electric fishing). We implemented restricted maximum likelihood

(REML) to treat the "sampling organisation" catchability factor as a random effect with a "flat" prior, so that it was not necessary to set this catchability factor to a given level when generating predictions with the fitted longfin eel models (Harville, 1974). It was assumed that longfin eel NZFFD data were collected using the standardised protocols of Joy et al. (2013), where each site was sampled by single-pass electric-fishing along a 150 m length of river.

### 2.3.2. Greater Waikato region electric fishing data

We also included longfin eel electric fishing catch data collected by the Waikato Regional Council (Charsley et al., 2021) in the present study. These data were collected in the greater Waikato region of New Zealand between 2009 and 2017. Every summer over this period, a subset of 101 sites throughout the greater Waikato region was sampled following the protocols outlined in Joy et al. (2013) (see Fig. A2). Seven "reference sites" were sampled every year from 2011 to 2017, and other sites sampled at varying frequencies. Longfin eel data were collected at each site by single-pass electric-fishing a 150 m length of river. The final longfin eel dataset contained information on eel count, body length, geographical coordinates and nzsegment. See Fig. A3 for longfin eel length and count distributions by year.

The data were further manipulated for use in VAST. To incorporate body length information into the VAST model, the data were categorised as smaller or larger than a specified "cut-off" length. Hence, every site was associated with a count for each length category. The count data were converted into counts per sampled river length (i.e., catch numbers/m).

### 2.4. Covariate data

The REC database includes New Zealand river geography information based on river, climate, topography, geology and land cover variables (Snelder and Biggs, 2002; Snelder et al., 2004). It also identifies large barriers (e.g., dams, weirs) that may prevent the migration of longfin eel up- and down-stream, and river access. These can be directly incorporated into models. Dams and river access are particularly important issues to consider in longfin eel SDMs (Hoyle, 2016).

The REC covariates *Mean flow* (cubic metres per second), *Distance to coast* (km), *Mean elevation* (m), *Mean slope* (degrees), *CV of annual catchment rainfall* (mm), *Mean January air temperature* ( $^{\circ}$ C  $\times$  10), and *Years since dam* were investigated as habitat covariates (Table 2) and were modelled as linear fixed effects in the VAST stream network models. All covariates, except the *Years since dam* covariate, are static (in that they do not change with time) and were selected based on known habitat preferences of New Zealand longfin eels (Crow et al., 2014; Jowett and Richardson, 1995, 1996; McDowall, 1990). Covariates were standardised to have mean zero and standard deviation one which implies that a covariate times its coefficient, i.e.,  $\gamma X$  in Eq. (1), has a standard deviation equal to the coefficient  $\gamma$  (Grüss et al., 2020a; Thorson, 2015). Covariates were explored for outliers and when

**Table 2**

Description of the covariates from the River Environment Classification (REC) database used in the present paper.

Name	Description
Mean flow (cumecs)	Mean annual river flow (cubic metres per second)
Distance to coast (km)	Downstream distance to the coast (km)
Mean elevation (m)	Mean elevation (above the sea level) of the watershed or basin (m)
Mean slope (degrees)	Mean slope of the watershed or basin (degrees)
CV of annual catchment rainfall (mm)	Coefficient of variation of annual catchment rainfall (mm)
Mean January air temperature ( $^{\circ}$ C $\times$ 10)	Average air temperature in January within section ( $^{\circ}$ C $\times$ 10)
Years since dam	The number of years since the construction of a downstream dam has been completed. It is set to zero if the dam is located upstream or if there are no dams.

necessary, transformed to have approximate normal distributions. Thus, the covariate *Mean flow* had a large positive skew and was, therefore, log transformed prior to standardisation.

### 2.5. Longfin eel case studies

The first two case studies modelled encounter/non-encounter data and catch rates in catch numbers/m to estimate, respectively, probability of encounter in the Waitaki catchment and numerical density in the greater Waikato region. The third case study used a simulation experiment to determine data requirements for estimating trends in female spawning biomass with a certain level of accuracy and precision and a good representation of uncertainty.

#### 2.5.1. Probability of encounter model for the Waitaki catchment

The NZFFD was used as a source of encounter/non-encounter data for the Waitaki catchment (2030 records covering the period 1960–2018; Fig. A4). Electric fishing was the only fishing method considered, to reduce the number of parameters estimated. A catchability covariate was included in the model to account for differences in catchability between sampling organisations. For example, organisations such as Fish & Game may have a lower catchability for longfin eel than the Department of Conservation (DOC), because Fish & Game tend to target non-native angling species such as trout when sampling, whereas DOC are more likely to target native species such as eels. The REC database was employed as a source of stream network information for the Waitaki, as well as a source of habitat covariates (Figs. A5 – A11). All the habitat covariates described in Table 2 were used in the spatio-temporal model. The Waitaki dam, which finished construction in 1934, defined the *Years since dam* habitat covariate.

A probability of encounter model was established in VAST by using a logit-link function to form a logistic regression while "switching off" the parameters associated with the second linear predictor". The model is a single-species model and, therefore, uses a single category ( $c_i$  can be ignored in Eq. (1)). The temporal component of the model was included as a random effect that was a random walk among years. This setting allowed temporal autocorrelation to be accounted for in the model. Spatial variation was included in the spatio-temporal model, but spatio-temporal variation was not, because the model failed to converge when spatio-temporal variation was modelled. The predictions from the model were used to produce probability of encounter maps, as well as estimates of effective river length occupied, for each year of the study period.

#### 2.5.2. Density model that considers fish length classes for the greater Waikato region

We developed a longfin eel density model with body length classes for the greater Waikato region. This model relied on standardised electric fishing data collected by the Waikato Regional Council between 2009 and 2017. The REC database was used to construct a stream network for the greater Waikato region and as a source of habitat covariates. All habitat covariates described in Table 2 were initially included in the spatio-temporal model. However, the model ultimately included only the effects of *Distance to coast* (km), *Mean elevation* (m) and *Years since dam* (Fig. A12 – A14). The gradients of the maximum likelihood estimated effects of *Mean flow*, *Mean slope*, *CV of annual catchment rainfall* and *Mean January air temperature* were all large (greater than 0.01) and therefore inestimable. These were, therefore, dropped from the model. The Karapiro dam, which finished construction in 1947, defined the *Years since dam* habitat covariate.

The model considered a single species but numerical catch rate data were classified into two length classes, determined by a cut-off length of 250 mm. In this case two categories were used to distinguish between eels  $<$  250 mm in length and  $\geq$  250 mm in length. This cut-off separated the data approximately evenly while grouping larger longfin eels together and all smaller eels together. A number of length cut-offs were explored, yet the 250-mm cut-off resulted in a converged model whilst

allowing for sufficient data in each category-site-year group.

The distribution model used for the greater Waikato region case study was the “Poisson-link delta model” (Thorson, 2018), which converged and fitted better than the classic delta model when modelling catch rate data for two length categories. The Poisson-link delta model employs the complementary log-log link function instead of the logit link function to express probability of encounter in the first linear predictor; for more technical details see Thorson (2018) and Grüss et al. (2021b).

The spatio-temporal model for the greater Waikato region was built using one factor for each of the spatial and spatio-temporal variation terms in the two linear predictors. Although the general guidance on factor modelling with the VAST modelling platform is to use the same number of factors as there are categories in the model (i.e., two in this case) (Thorson, 2019a), we decided to only use one factor so that the number of estimated parameters was reduced and the spatio-temporal model would converge, given the relatively sparse dataset. Using one factor implies that each site has a different magnitude of response to a single estimated spatial or spatio-temporal process.

Temporal components of the spatio-temporal model were modelled as random effects, assuming a random walk among years. The spatial and spatio-temporal variation terms were estimated in the model, and the spatio-temporal variation term was assumed to be autoregressive among years. Under these settings, the model converged, which allowed for spatial, temporal and spatio-temporal autocorrelation to be accounted for. Predictions from the model were used to produce density maps, as well as estimates of effective river length occupied, for each year of the study period.

### 2.5.3. Simulation experiment

Finally, we conducted a simulation experiment to determine data requirements for estimating trends in longfin eel female spawning biomass with a certain level of accuracy and precision and a good representation of uncertainty. This last case study used the “bootstrap simulator” included in R package VAST (Thorson, 2019a). We designed operating models (OMs) similar to the model in the previous case study (Subsection 2.4.2). Conditional on the maximum likelihood estimates of the fixed effects from the OMs, new random effects and new data were simulated. These new data were then fitted with an estimation model (EM), and the index of abundance estimated by the EM was compared to the “true” index of abundance to determine the accuracy, error and confidence interval coverage associated with the sampling protocol assumed to generate the simulated data.

Two OMs were built, consisting of time series of 9 and 20 years. Both OMs were based on numerical catch rate and length data collected in the greater Waikato region. As a proxy for female spawning biomass, we categorized body lengths as above (or equal to) and below 500 mm. Mean length at migration for longfin eel males has been estimated as 620 mm (Hoyle and Jellyman, 2002). Therefore, longfin eels larger than 500 mm may include some males but are more likely to be female than male. Cut-off lengths larger than 500 mm were trialled, including a cut-off of 620 mm, but in these cases, there was not enough data in the upper group for parameters to be estimated.

The 9-year OM was built with temporal components estimated as yearly fixed effects. Using fixed effects allowed the year effect to be altered when simulating data, whereas a random effect is based around a mean value and values cannot be specified for a simulation. Data were simulated by adding an additional 60 sampling sites for each category (i.e., 120 records) and for each year, i.e., a total of 1080 records, to the greater Waikato region. These sites were included in the model likelihood so that data could be simulated at these sites. Additional sites were sampled based on how likely the sampler was to encounter a longfin eel at the site. This guided a more realistic sampling scheme in which sites are visited based on access and with some consideration of the likelihood of catching longfin eel, among other factors. Therefore, longfin eel probability of encounter was predicted in the greater Waikato region

using an independent method. In this case using a Regularised Random Forest (RRF) model. Sites with RRF probability of encountering a longfin eel greater than 0.68 (the upper quarter of the RRF probability of encounter predictions for that area) were randomly sampled. The OM assumed these sites were resampled each year.

The 9-year OM used a single factor for each of the spatial and spatio-temporal variation terms in the two linear models to reduce the number of parameters to be estimated. The spatio-temporal variation term was set to be autoregressive among years. This setting allowed temporal correlation in longfin eel density hotspots to be estimated (Thorson, 2019a) and, therefore, allowed for a more realistic account of longfin eel population density. The 20-year OM was built identically to the 9-year OM, except that sampling was projected for an extra 11 years (20 years in total (2009–2028)). Projecting into the future required the temporal component to be modelled as a random effect.

When simulating data, we investigated four scenarios for the 9-year and 20-year time series. First, the annual sample size was simulated as either  $n = 15$  or  $n = 30$ , and second, the trend was either kept the same as in the OM ( $\text{tre} = 0$ ) or altered so that the time series declined by approximately 50% over the time period ( $\text{tre} = 1$ ). See Fig. A15 for more details. One hundred datasets were simulated from the 9-year and 20-year time series for each scenario, i.e., a total of 800 datasets were simulated.

The EMs were also built using VAST. They included no spatio-temporal term and used a single factor for the spatial term in the two linear predictors. These settings were necessary to reduce the number of estimated parameters and ensure that the EMs converged. The temporal component was assumed to follow a random walk among years, which resulted in higher rates of model convergence compared to when the temporal component was tested as independent among years. Failed EMs were re-run without habitat covariates to reduce the number of parameters estimated.

Several performance metrics were calculated for each simulation scenario. First, to determine the accuracy of the assumed sampling protocols, we calculated: (1) the slope of the regression between the estimated annual index of abundance and year, and the slope of the relationship between the “true” annual index of abundance and year, and used the difference between the two slopes as an index of reliability for the estimated trend (the closer to zero the better); (2) annual absolute bias, given by the estimated annual index of abundance minus the “true” annual index of abundance; and (3) annual relative bias, given by the annual absolute bias divided by the “true” annual index of abundance. Then, to determine the error of the assumed sampling protocols, we calculated root mean square error (RMSE; the lower the better; (Stow et al., 2009)). Finally, to determine whether the assumed sampling protocols resulted in more or less well-calibrated confidence intervals, we computed coverage for a 50% confidence interval (“coverage”; Bolker, 2008; Grüss and Thorson, 2019). Coverage is the percentage of years that the 50% confidence interval of the estimated index of abundance contains the “true” index of abundance. Coverage values greater than 50% indicate that confidence intervals are too wide, whilst coverage values smaller than 50% indicate that confidence intervals are too narrow (Bolker, 2008; Grüss et al., 2019b; Johnson et al., 2016). We also recorded the percentage of replicates where the EM failed to converge.

## 3. Results

### 3.1. Probability of encounter for the Waitaki catchment

The first model was developed for longfin eel in the Waitaki catchment using NZFFD encounter/non-encounter electric fishing data. The model was initially trialled with a spatio-temporal variation term. However, spatio-temporal variation was found to be negligible (i.e., was estimated to be close to zero), so the spatio-temporal variation term was dropped from the model (Table A16). The negligible estimated effect of

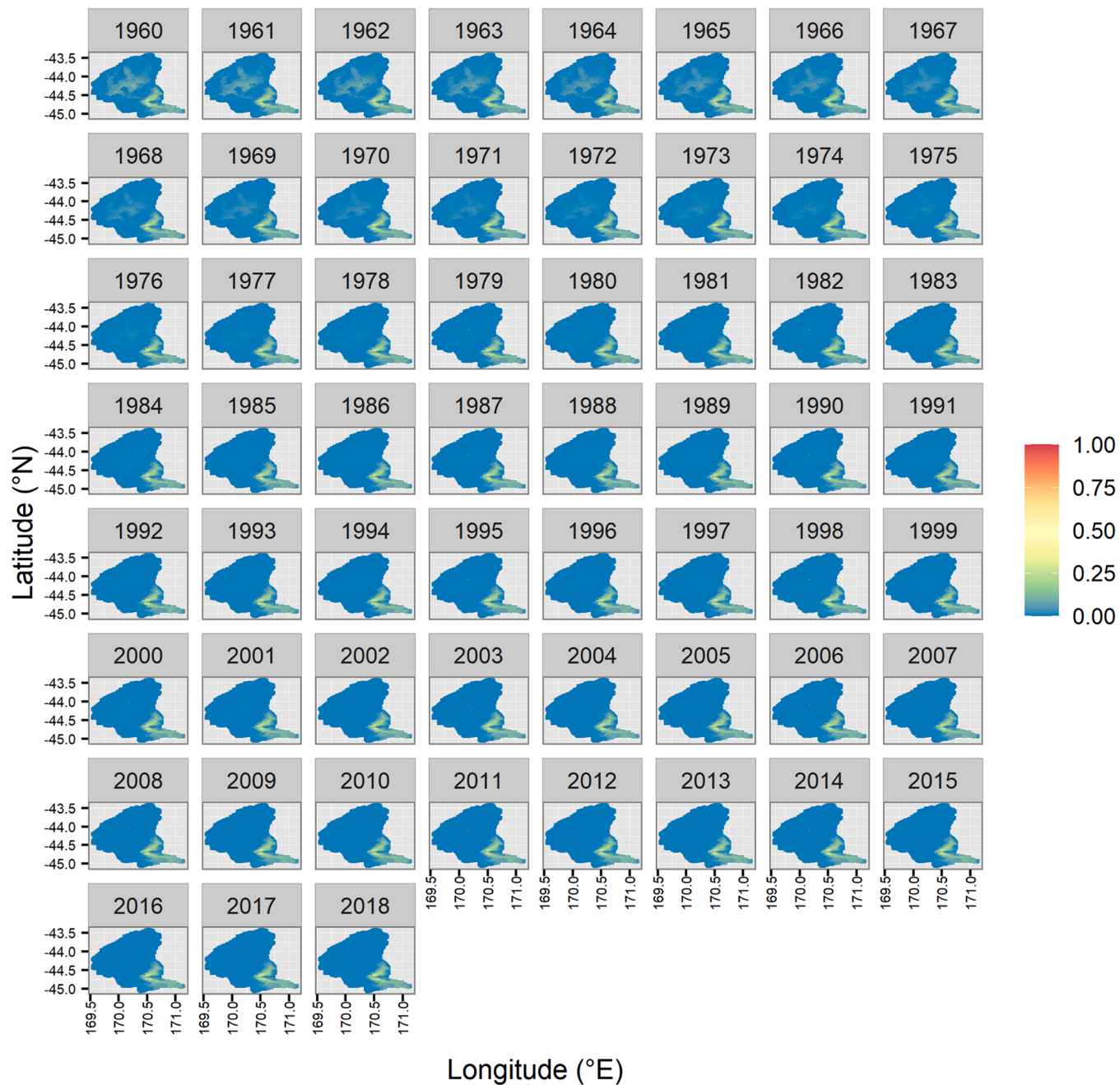


**Fig. 2.** Probability of encounter maps for longfin eel (*Anguilla dieffenbachii*) predicted by the spatio-temporal model fitted to encounter/non-encounter data for the Waitaki catchment.

the spatio-temporal variation term was very likely due to the very low percentage of encounter data available for the case study (4%; Fig. A4). Encounters were mainly observed in the same low latitudes and high longitudes (of the study area i.e., close to the river mouths) across time (Fig. A4).

The DHARMA residuals were approximately normally distributed (Fig. A17) and were evenly distributed between zero and one (Fig. A18). Values of one indicate that the observed value is greater than all the simulated values; these were rare. The DHARMA residuals appeared to be approximately evenly distributed across low and high values across space and time (Fig. A19). This indicates approximate independence in the model residuals.

The probability of encountering longfin eel was predicted to be very small throughout most of the Waitaki catchment (Fig. 2). The highest probabilities of encounter were generally predicted for the low latitude/

high longitude areas of the catchment (i.e., close to the river mouths) and ranged between 0.1 and 0.4, except between 1960 and 1966 where they were predicted to occur in the centre of the Waitaki catchment. The estimated temporal effect was very small (Table A16). This was reflected in the probability of encounter maps estimated by the model, which showed very little change in longfin eel probability of encounter over time (Fig. 2).

The estimated effective river length occupied decreased exponentially, reaching a relatively stable level by about 1990 (Fig. 3). However, the 95% confidence intervals associated with effective river length occupied estimates were large, i.e., effective river length occupied predictions were uncertain (Fig. 3).

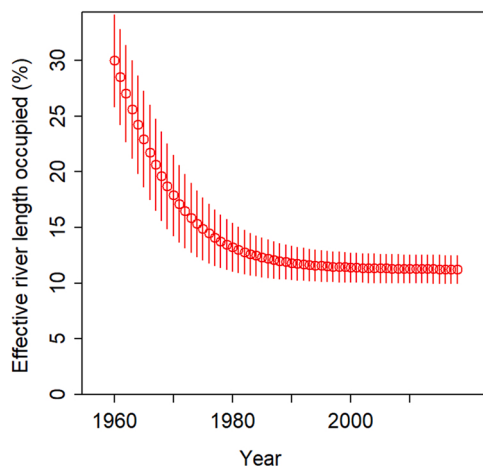


**Fig. 3.** The effective river length occupied by longfin eel (*Anguilla dieffenbachii*) in the Waitaki catchment across time, predicted by the probability of encounter model developed in the present study.

### 3.2. Density by length class for the greater Waikato

The longfin eel density model for the greater Waikato region used electric fishing catch rate data collected by the Waikato Regional

Council for two length categories (shorter or longer than 250-mm). The Waikato Regional Council surveys encountered longfin eels throughout the greater Waikato region but observed catch rates tended to be higher at lower latitudes and longitudes (i.e., close to the southwest river mouths), particularly in the < 250-mm length category (Fig. 4).

DHARMA residuals appeared to be evenly distributed between zero and one across space and time and to be independent (Fig. A20 and Figs. A21 and A22). A closer inspection of the DHARMA residuals (Figs. A21 and A22) revealed a slight peak around 0.5 suggesting underdispersion, but this deviation from the expected distribution was minimal.

The model predicted density to be relatively constant throughout the study period in both length categories (Figs. 5 and 6). This result is associated with very small estimates for the loadings scalar parameters that generate temporal variability (Table A23). Longfin eels less than 250 mm were predicted to be densely distributed at low latitudes and longitudes (close to river mouths in the south-west catchment) and to be less densely distributed in the rest of the stream network, apart from some high densities predicted further north (central catchment and northeast river mouths) (Fig. 5). Longfin eels equal to or longer than 250 mm were predicted to be densely distributed throughout the study stream network, with density hotspots in low longitude areas across low to high latitudes (close to the river mouths along the west coast) (Fig. 6).

The estimated effective river length occupied by longfin eels (both <250-mm-long and  $\geq 250$ -mm-long) was stable across time, with a

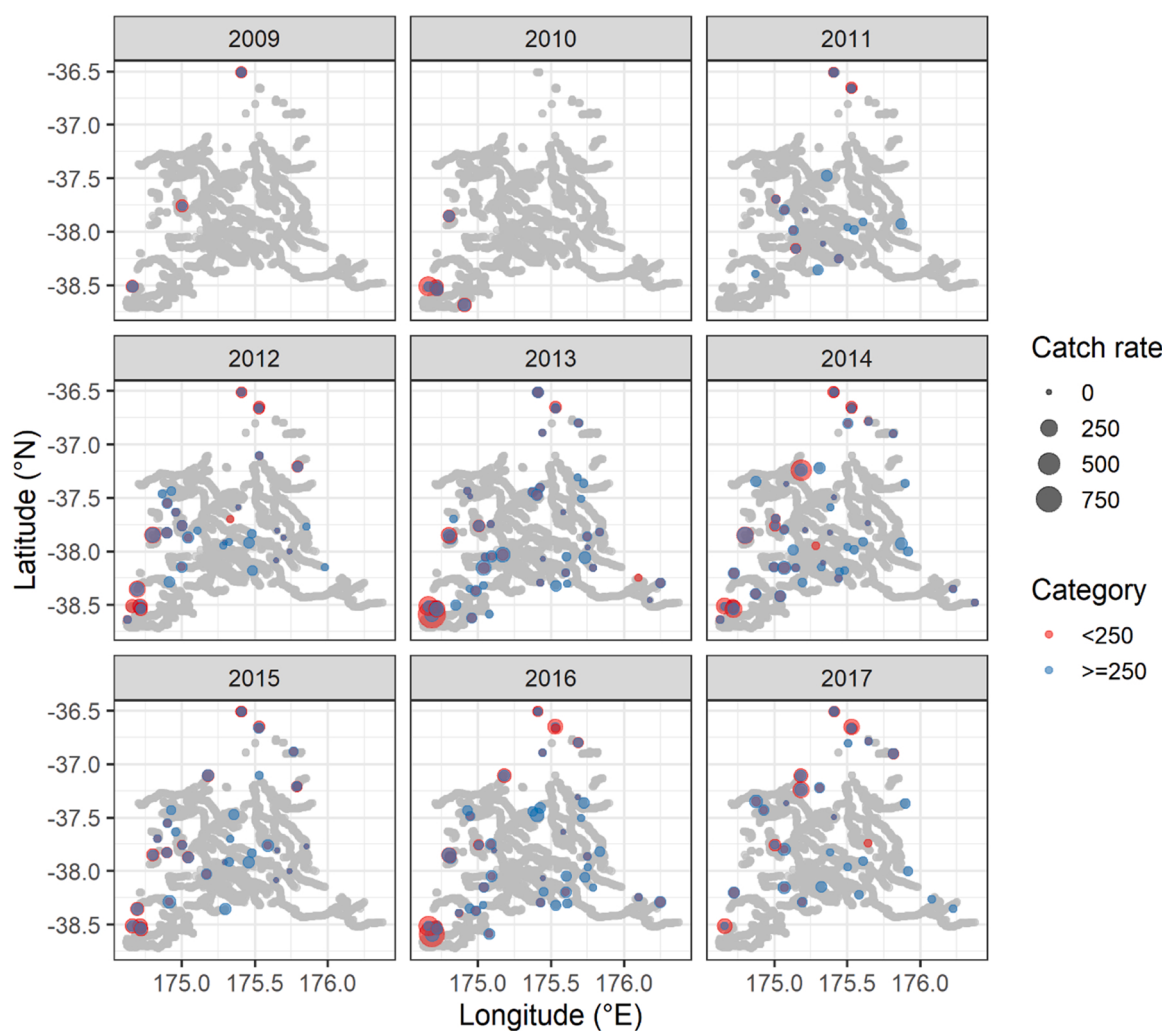


**Fig. 4.** Longfin eel (*Anguilla dieffenbachii*) catch rates (counts per 150 m of river) in the greater Waikato region by year. These data were collected by the Waikato Regional Council using standardised electric fishing.

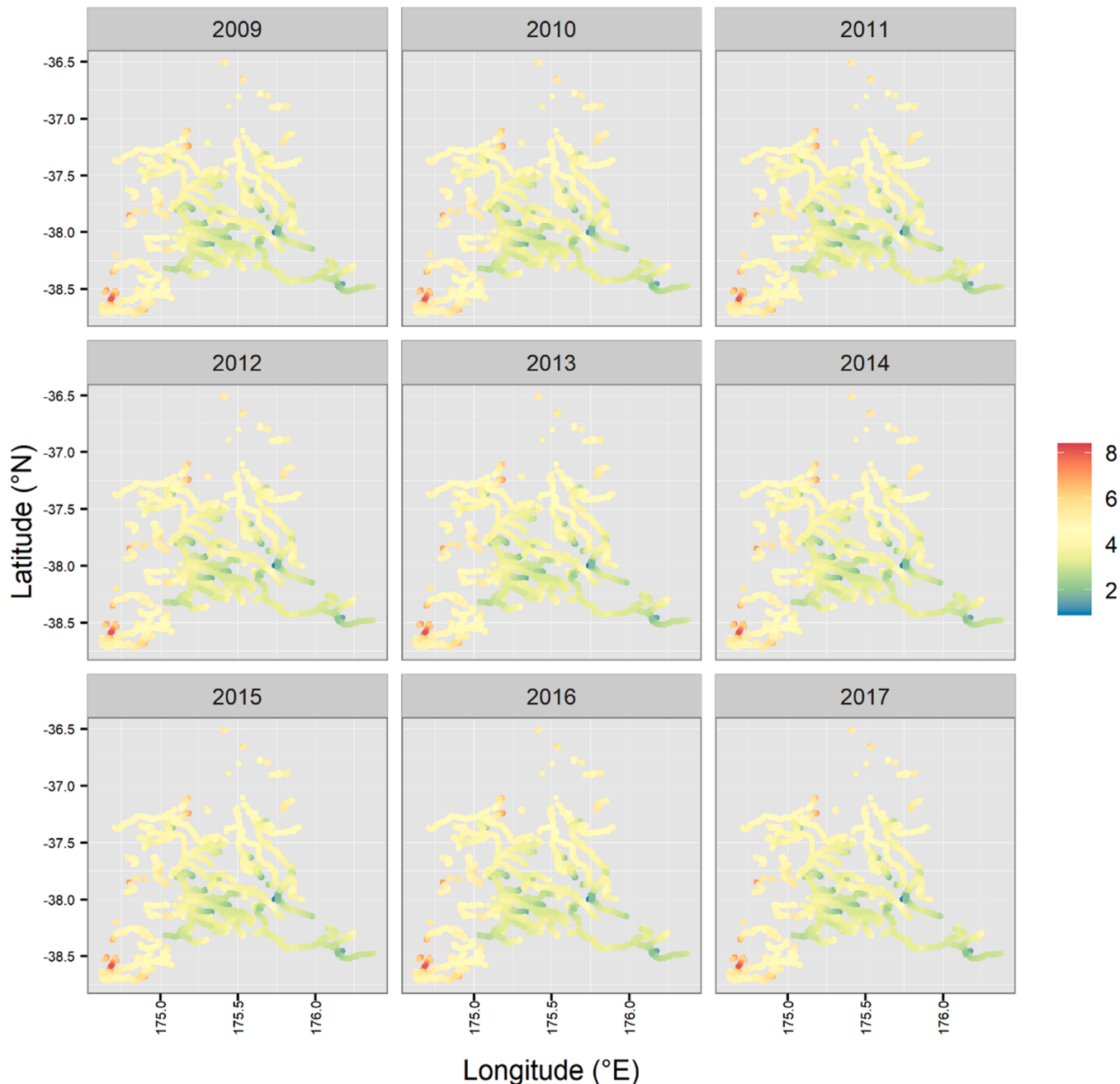


**Fig. 5.** Log density ( $\log(\text{count}/\text{km})$ ) maps for < 250-mm long longfin eel (*Anguilla dieffenbachii*) predicted by the spatio-temporal model fitted to catch rate data for the greater Waikato region.

higher effective river length occupied by  $\geq 250$ -mm-long longfin eels (Fig. A24). The probability of encounter of both longfin eel length categories was predicted to slightly decrease in response to the implementation of the Karapiro dam, while their non-zero densities were predicted to slightly increase (Table A23).

### 3.3. Simulation experiment

Model fits for the 9-year and 20-year OMs showed a slightly higher frequency of DHARMA residuals around 0.5 (Fig. A25 – A30), which indicated a very small amount of underdispersion. Models were first run with all available habitat covariates, and models that failed to converge were re-run without habitat covariates. Most EMs converged and estimated longfin eel abundance indices successfully for the 9-year time period (Table A31). We were able to estimate all indices for the 20-year

time period after the two attempts.

For the 9-year simulations, the trend estimates were generally unbiased, apart from some positive bias for the declining scenario (50% over the time period) with 15 samples per year, with the median slope approximately 0.01 per year (Fig. 7). For both trend scenarios, uncertainty in the trend estimates was similar at the same sample size, but with considerably more precision at the higher sample size of 30 per year (Fig. 7).

The coverage metric suggested that the confidence interval estimates were too wide for the 9-year simulations (Figs. A32 – A35, top left plots). For a 50% confidence interval, it was expected that the simulation experiment would have found that the true metric was within the estimated confidence interval 50% of the time. In all the 9-year simulations, the coverage was greater than 50%. The coverage estimates assume that the density estimates are independent of one another, which is not the

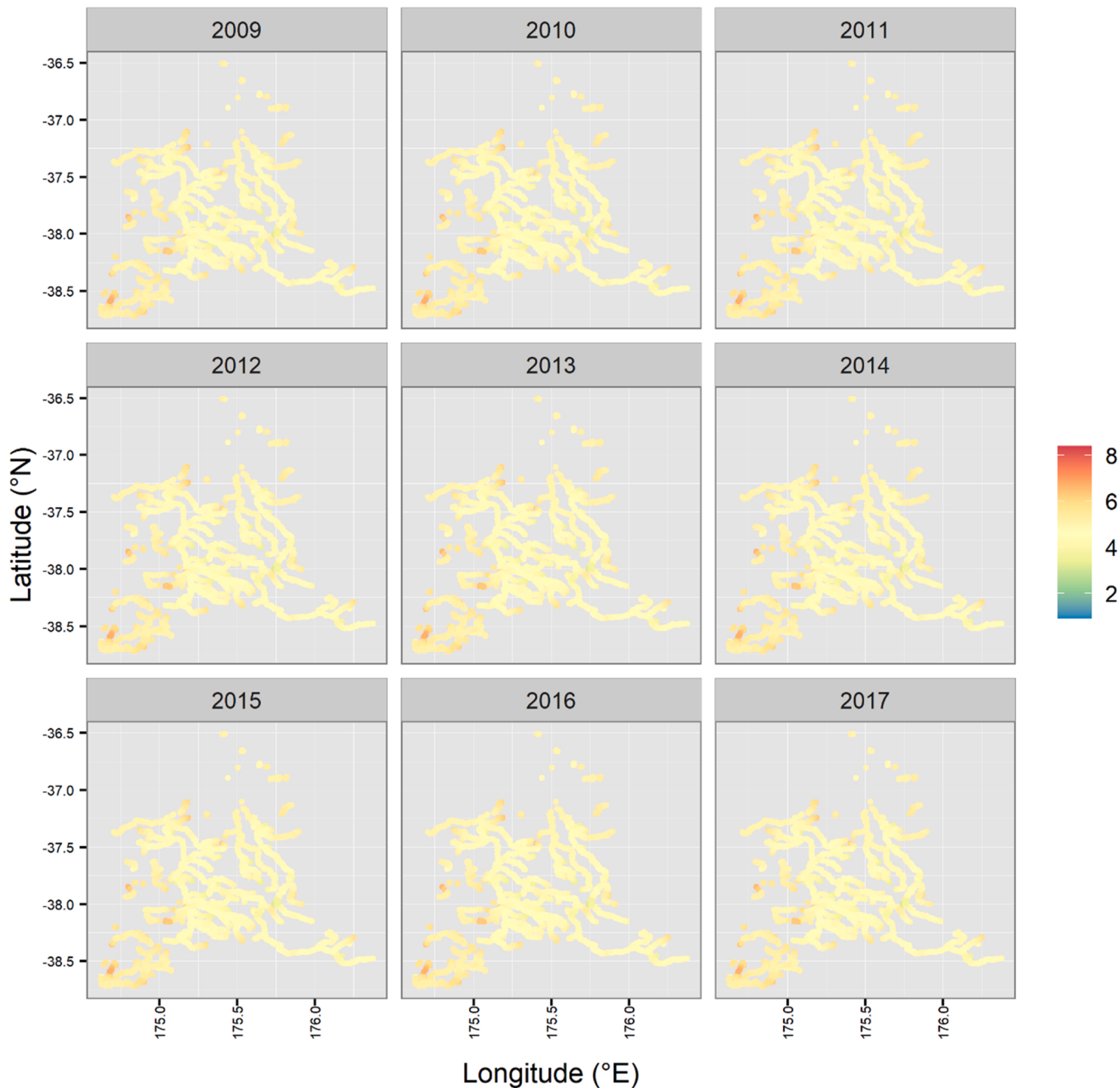


**Fig. 6.** Log density ( $\log(\text{count}/\text{km})$ ) maps for  $\geq 250\text{-mm}$  long longfin eel (*Anguilla dieffenbachii*) predicted by the spatio-temporal model fitted to catch rate data for the greater Waikato region.

case due to spatio-temporal correlation in the spatio-temporal model. Looking at results in terms of absolute and relative biases, estimates for the scenario with declining population density and 15 samples per year showed evidence of bias in the trend estimate (Figs. A34, bottom row), but this bias was absent from the equivalent scenario with 30 samples per year (Figs. A35, left and middle plots of the bottom rows).

For the 20-year simulations, the trend estimates appeared largely unbiased (Fig. 8), apart from slight positive bias for the scenarios with declining trend and 15 samples per year (Fig. 8, bottom-left plot). The coverage metric suggested that the confidence interval estimates were too wide for the 20-year simulations (Figs. A36 – A39, top left plots) because, in almost all cases, the coverage was greater than 50%. Some positive bias in annual estimates was evident for the scenarios with declining population density and with both 15 and 30 samples per year (Figs. A38 and A39, bottom row).

#### 4. Discussion

This study developed and applied a novel spatio-temporal modelling framework for stream networks based on the VAST platform and the Ornstein-Uhlenbeck algorithm. This framework is referred to as the “VAST stream network modelling framework”. The two real-world applications presented here demonstrate how the VAST stream network modelling framework can provide useful information to freshwater resource managers, including insights into spatio-temporal changes in the distributions of different fish length classes and estimates of effective river length occupied. The simulation experiment showed that our modelling framework can also be employed to evaluate the performance of alternative sampling scenarios in monitoring trends in fish spawning biomass.

The VAST stream network modelling framework represents a more

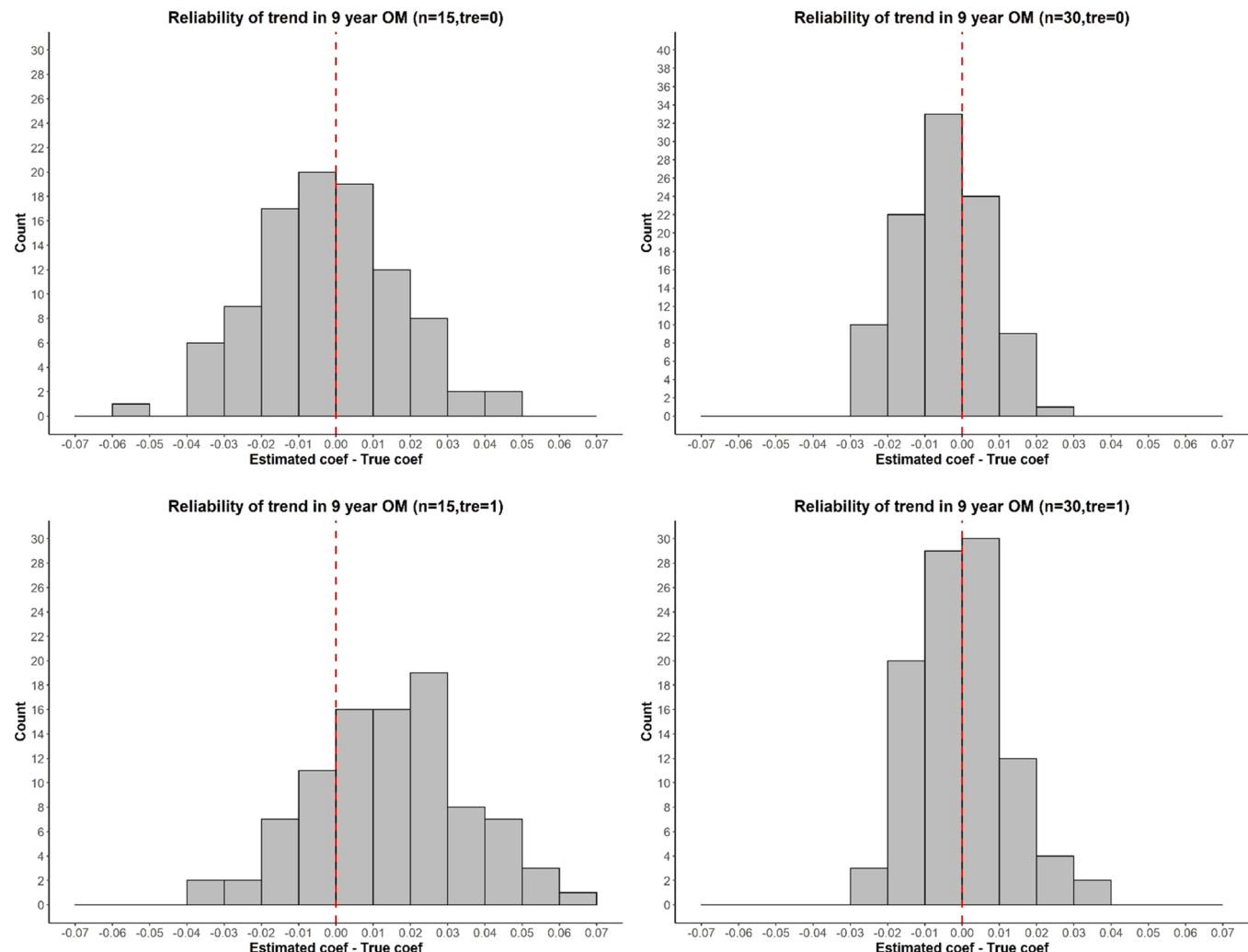


**Fig. 7.** Reliability of the estimated trend for the 9-year operating model (OM) in the simulation experiment, with a sample size of 15 per year (left panels) and 30 per year (right panels), when trend parameters are unchanged (top panels) or a 50% decline over 20 years is assumed (bottom panels). For details about the simulation experiment, the reader is referred to the main text. The reliability metric is given by the difference between the slope coefficient of the regression between the estimated annual index of abundance (given by the estimation model) and year and the slope coefficient between the “true” annual index of abundance (given by the OM) and year.

realistic, precise, and useful tool for modelling populations of freshwater species than the modelling methods previously used for this purpose (e.g., for longfin eel: [Crow et al., 2014](#); [Crow et al., 2016b](#); [Graynoth and Booker, 2009](#); [Graynoth et al., 2008](#); [Graynoth and Niven, 2004](#); [Joy et al., 2018](#); [Leathwick et al., 2008](#)). Our modelling framework allows quantities of interest (e.g., probability of encounter, fish density and effective river length occupied) to be estimated while accounting for spatial and spatio-temporal variation ([Hocking et al., 2018](#)), as well as habitat and catchability variables that explain some of the remaining variance in the data ([Thorson, 2019a](#)). As with any modelling tool, caution must be taken when interpreting derived quantities. For example, effective river length occupied is useful for giving an overall view of species occupation in the catchment. However, the quantity is derived over all rivers in the catchment, including wide rivers such as lower estuary rivers. In these rivers, effective river length occupied is less accurate because species occupation will likely change across length and width. Nevertheless our modelling framework improves over previous methods by: (1) providing a time series of predictions across space; this is particularly an advantage over machine learning methods (often used in freshwater fish modelling), which, given their many hidden parameters and interaction terms, are difficult to constrain into a plausible parameter space when predicting beyond the spatio-temporal

range of the training data; (2) being able to integrate information such as counts, body lengths and sex composition of the catch, so that the estimated indices of abundance more closely approximate spawning biomass; and (3) accounting for the length of time instream barriers (dams and weirs) have been present through the use of a specific *Years since dam* covariate.

Although our stream network spatio-temporal modelling framework is novel, this is not the first time that VAST has been employed to model the distribution of freshwater fishes. Previous VAST models estimated the relatedness between points in space based on Euclidian distance rather than distance within the stream network ([Charsley et al., in press](#)). These models aimed to understand the spatial distribution patterns of longfin and shortfin eels at the scale of New Zealand. Computation costs are much higher for analyses that relate points in space using stream networks than for analyses using Euclidean distances and calculating stream network spatial connections for all of New Zealand was not feasible ([Charsley et al., in press](#)). However, the Euclidean distance model performed poorly at smaller spatial scales (e.g., the Waitaki catchment) (see [Ver Hoef et al., 2006](#) for further discussion). Potentially, the stream network modelling framework could be further developed to allow a reduction in the complexity of the network ([Charsley et al., in press](#)). For example, [Charsley et al., in press](#) suggests

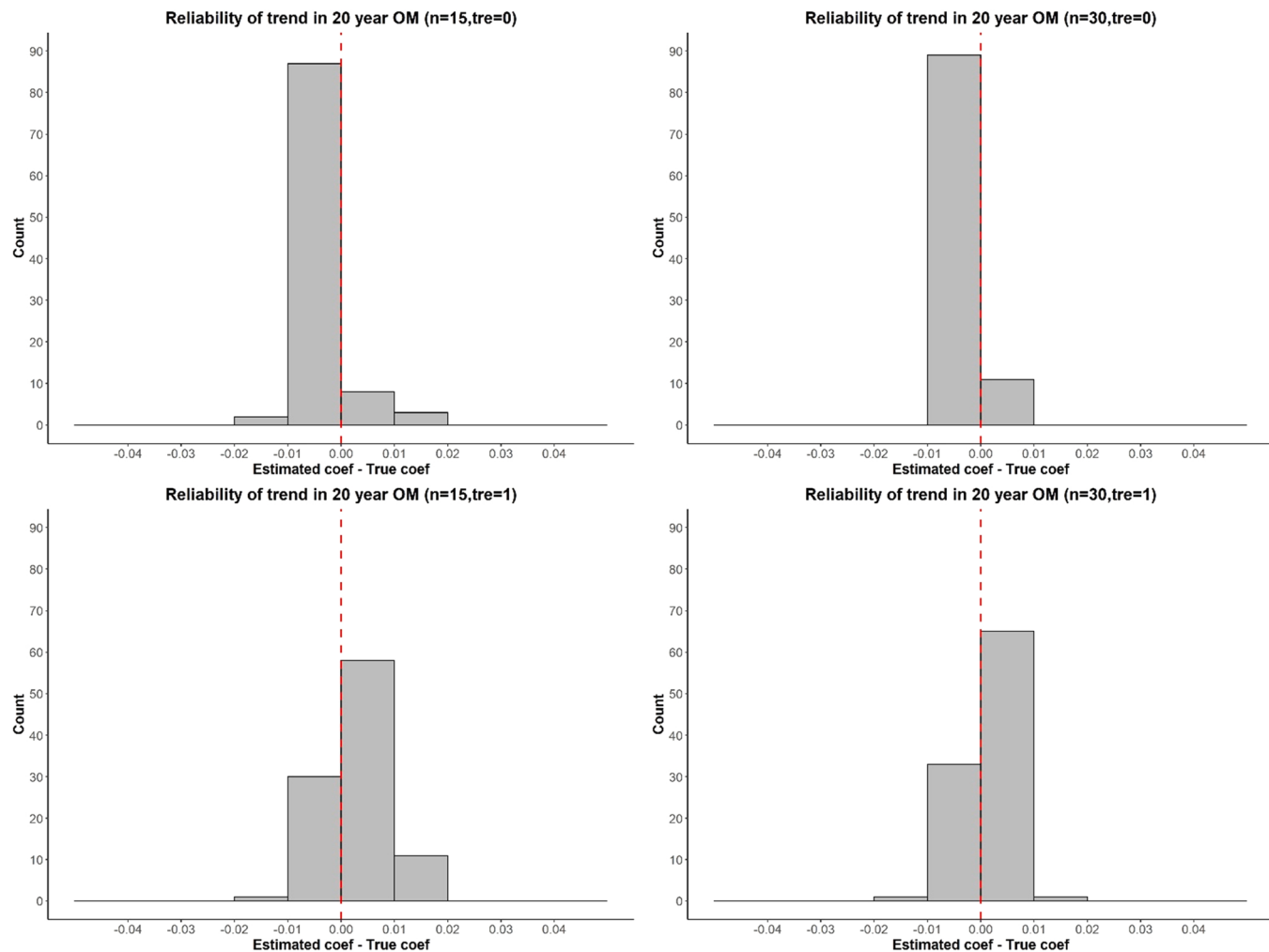


**Fig. 8.** Reliability of the estimated trend for the 20-year operating model (OM) in the simulation experiment, with a sample size of 15 per year (left panels) and 30 per year (right panels), when trend parameters are unchanged (top panels) or a 50% decline over 20 years is assumed (bottom panels). For details about the simulation experiment, the reader is referred to the main text. The reliability metric is given by the difference between the slope coefficient of the regression between the estimated annual index of abundance (given by the estimation model) and year and the slope coefficient between the “true” annual index of abundance (given by the OM) and year.

that aggregation of certain river segments to reduce the overall size of the network would allow population-level models to run at a lower computational cost. Moreover, our VAST stream network modelling framework builds upon SSN models (Cressie et al., 2006; Isaak et al., 2014, 2016; Ver Hoef et al., 2014, 2006; Ver Hoef and Peterson, 2010) which also account for spatial autocorrelation within a stream network. However, unlike VAST, the covariance structures of SSN models do not incorporate spatial and temporal autocorrelation simultaneously (Isaak et al., 2014). Including both spatial and temporal autocorrelation is an important improvement, as it provides better trend estimates through space and time for freshwater resource managers. This, as well as further developing the stream network feature at the species distribution range, could provide useful insights into longfin and shortfin eel populations and potentially inform population assessment.

Time series and catchment-specific results are particularly valuable to freshwater resource managers. Previous machine learning methods (Leathwick et al., 2008; Crow et al., 2014) did not estimate time series of probability of encounter for specific catchments, but instead produced a single map, thereby ignoring the temporal aspects of the data. These studies, as well as Charsley et al. (in press) and Crow et al. (2016a), also estimated statistical associations at a national scale rather than at a catchment scale. Charsley et al. (in press) used a standard Euclidean-space VAST model with a spatial mesh to estimate spatial and

spatio-temporal variation at the vertices of this mesh (Thorson et al., 2015). Then, spatial and spatio-temporal variation and, therefore, probability of encounter were predicted over the whole study area using spatial interpolation (Grüss et al., 2020a). There was then a “transferability” issue where predictions could not be made at a very fine spatial resolution, as the estimation of spatial and spatio-temporal autocorrelation was based on data points that were mostly very far from one another (Grüss et al., 2021a). Thus, Charsley et al. (in press) was unable to predict probabilities of encounter in the Waitaki catchment, but still managed to estimate low (0–0.4) probabilities of encounter for locations close to the Waitaki catchment for the period 1974–2014. This result is consistent with the present study, as well as Leathwick et al. (2008) and Crow et al. (2014), all of which predicted low probabilities of encounter (0–0.4) for the Waitaki catchment. However, the results from earlier studies are less reliable and useful for the Waitaki catchment because they have substantially less spatial and/or temporal resolution and do not account for habitat covariate relationships at the catchment scale.

The second real-world application presented in this study, for the greater Waikato region, was able to jointly model two categories: juvenile eels (“elvers”) and larger eels. VAST models of multiple categories can improve model predictions, as shown by Thorson and Barnett (2017) who found that a joint species distribution model for eight US

Pacific Coast species was more parsimonious and achieved better predictive performance than single-species models. This approach may have particular benefits for body size categories of a single species, when the presence of one body size class indicates the potential for others to be present. Splitting the dataset into categories can be useful when habitat requirements change with body size, or when information about a particular category is required. The present study was constrained by the need for sufficient data in each body length category to achieve model convergence. Larger datasets will accommodate more body length categories, such as < 250-mm, 250–500 mm and > 500-mm, to permit for the estimation of both recruitment (elvers) and female spawning biomass. Future research could also explore the potential improvements (i.e., model parsimony and predictive performance) of univariate versus multivariate stream network spatio-temporal models. In addition, models that distinguish between males and females in each length category may provide more reliable advice about female spawning biomass, although this requires sex-specific data which is currently not widely available. Additionally, joint species distribution models where the categories are different species (and possibly different species body length categories as well) could be explored. For example, banded kōkopu (*Galaxias fasciatus*) and shortjaw kōkopu (*Galaxias postvectis*) represent important species in the New Zealand whitebait fishery, but data for them are extremely limited across New Zealand (Crow, 2018). More reliable predictions may be obtained by modelling them jointly with other species of the New Zealand whitebait fishery (Thorson and Barnett, 2017).

In addition to the two real-world applications, a simulation experiment was conducted in the present study to understand the performance of sampling scenarios in monitoring trends in fish spawning biomass. As expected, a longer time series enhanced the precision and the reliability of trend estimates, and increasing the annual sample size resulted in precise and largely unbiased estimates for the declining trend scenario (a common scenario for freshwater fishes). Importantly, a decline in female spawning biomass of 50% over the time series was detected, precisely and with only slight positive bias, with only nine years of data and 30 sites sampled. However, the simulation experiment assumed that the standardised sampling protocols of Joy et al. (2013) were followed and that samples were collected from river segments that were representative of the study area. Sampling schemes may ignore variables such as river habitat type, stream order and total size of river segments. Where ignoring these variables may introduce sampling bias which may impact estimates of abundance and effective river length occupied. Sampling bias was indirectly addressed in the simulation experiment by incorporating longfin eel encounter probabilities into the simulation experiment sampling scheme (i.e., sampling often occurs at sites where longfin eels are likely to be found). However, a comprehensive sampling scheme which directly incorporates variables that introduce sampling bias should be derived. We recommend that future simulation experiments examine the impact of habitat type, stream order and total size of river segment on sampling bias, and estimates of abundance and effective river length occupied.

Sampling data for longfin eel are currently available only for a few New Zealand catchments (Haro et al., 2015; Hoyle, 2016). Given the commercial, recreational, and customary importance of longfin eel, it is paramount to increase sampling across New Zealand. However, sampling is expensive so should be carefully designed to attain monitoring objectives while minimising costs. This is where simulation experiments are valuable, to help understand sampling performance under alternative scenarios regarding fish population trends, habitat features, and sampling specifics (Hoyle, 2016; Peterson et al., 2013; Isaak et al., 2016). Only a limited number of scenarios were considered in the present study and we, therefore, encourage future studies to conduct additional simulations for specific catchments or regions and to explore more scenarios regarding fish population trends and sampling specifics.

Our VAST stream network modelling framework currently has relatively high data requirements and may be well suited to studies of the

freshwater stages of data-rich eel populations such as the commercially exploited stocks in Europe, North America and Japan. In Europe, an Eel Density Analysis (EDA) model is currently being used to harmonise European eel predictions across Portugal, Spain, and France (Briand et al., 2022). The EDA model was established under the SUDOANG project, which aims to coordinate and standardise data, standardise management and assessment tools, and increase cooperation with stakeholders (Briand et al., 2022). There is potential to apply VAST stream network models to European eel data and make comparisons with the EDA model. Data requirements for employing our VAST stream network modelling framework include a model of the stream network, including linked habitat attributes, and time series of spatially referenced response variable data. Our modelling framework can handle multiple response variable sampling methods, representing sampling methods with different catchability. For example, one could use the VAST stream network modelling framework to develop an eel model incorporating data from electrofishing, fyke netting, and traditional knowledge (e.g., Jellyman and Graynoth, 2005; Shortland and Tipene-Thomas, 2019; Weldon et al., 2020). There is also great potential to include eDNA data, as a relatively cheap source of information with potential for widespread monitoring (Li et al., 2019; Weldon et al., 2020).

Beyond eels, our modelling framework is applicable to any freshwater species, including fishes, crustaceans, insects, and plants, or to attributes of freshwater systems such as diversity. For example, there is scope for our modelling framework to be applied to Atlantic salmon (*Salmo salar*) in Scotland. As a result of the National Electrofishing Programme for Scotland (NEPS) there is extensive spatial electrofishing data for Atlantic salmon and other freshwater fish populations (Malcolm et al., 2020). The VAST stream network modelling framework can be employed for a range of purposes, such as estimating the distributions of native species for conservation and habitat management, of fished species for fisheries management, or of invasive species to help with control.

In addition to the avenues for future research mentioned above, we envision several others. First, while VAST stream network models are more realistic for freshwater habitats than traditional VAST models estimating spatial relatedness based in Euclidian distance, the degree of improvement in estimates has not been demonstrated. Therefore, future research should compare the performance and predictions of the two approaches. Moreover, we recommend future studies to compare VAST stream network models with spatial GAMs, which represent broad-scale spatial autocorrelation using a tensor product smooth between eastings and northings (Grüss et al., 2021a). With respect to longfin eels, it would be advantageous to explore spatial GAMs for longfin eel populations to gain rapid insights into longfin eel trends in most of New Zealand stream systems.

In conclusion, we presented here a novel VAST stream network modelling framework together with two New Zealand case studies and a simulation experiment. These three applications and the Oregon coho salmon application (Rudd, pers. comm.) demonstrate the potential for VAST stream network modelling studies of freshwater species. The main issue for fitting VAST stream network models is the availability of sufficient data. To optimise the collection of sufficient data for freshwater species, we recommend thorough simulation experiments for stream network systems using our modelling framework, exploring diverse scenarios regarding fish population trends, habitat features and sampling specifics.

#### CRediT authorship contribution statement

**Anthony Charsley:** Methodology, Formal analysis, Data curation, Writing – original draft, Visualization. **Arnaud Grüss:** Methodology, Writing – original draft. **James T. Thorson:** Methodology, Software, Writing – review & editing. **Merrill Rudd:** Software, Writing – review & editing. **Shannan Crow:** Methodology, Writing – review & editing.

**Bruno David:** Data collection. **Erica Williams:** Conceptualization, Funding acquisition. **Simon Hoyle:** Conceptualization, Funding acquisition, Methodology, Writing – original draft.

## Funding

This work was supported in part by the New Zealand Ministry of Business, Innovation and Employment (MBIE) under the Cultural Keystone Species Programme (CO1X1616) awarded to the National Institute of Water and Atmospheric Research (NIWA), and by the New Zealand Ministry for Primary Industries under project EEL201701. The funders had no role in study design, data collection and analysis, decision to publish, or preparation of the manuscript.

## Declaration of Competing Interest

The authors declare that they have no known competing financial interests or personal relationships that could have appeared to influence the work reported in this paper.

## Data Availability

Data will be made available on request.

## Acknowledgments

We thank the Fisheries New Zealand eel working group for their useful feedback on the draft manuscript. We thank the New Zealand Ministry of Business, Innovation and Employment (MBIE), Fisheries New Zealand (FNZ), and the National Institute of Water and Atmospheric Research (NIWA) for funding this research. We thank Marc Griffiths at FNZ who secured funding along with catch data from Waikato Regional Council so that the present project could be completed. We also thank Brad Moore, Brandon Chasco and Daniel Hocking, as well as two anonymous reviewers, for their comments which improved the quality of the manuscript.

## Appendix A. Supporting information

Supplementary data associated with this article can be found in the online version at [doi:10.1016/j.fishres.2022.106583](https://doi.org/10.1016/j.fishres.2022.106583).

## References

- Bolker, B.M., 2008. *Ecological Models and Data* in R. Princeton University Press, Princeton.
- Booker, D.J., Graynoth, E., 2013. Relative influence of local and landscape-scale features on the density and habitat preferences of longfin and shortfin eels. *N. Z. J. Mar. Freshw. Res.* 47 (1), 1–20.
- Briand, C., Maria, M., Drouineau, H., Maria, K., Estibaliz, D., Laurent, B., 2022. Eel Density Analysis (EDA 2.3). Escapement of silver eels (*Anguilla anguilla*) from French, Spanish and Portuguese rivers. GT4-deliverable E4. 1.1. Retrieved from (<https://hal.archives-ouvertes.fr/hal-03590458>).
- Burnham, K.P., Anderson, D., 2002. *Model Selection and Multi-Model Inference*, Second ed., Springer, New York.
- Cao, J., Thorson, J.T., Richards, R.A., Chen, Y., 2017. Spatiotemporal index standardization improves the stock assessment of northern shrimp in the Gulf of Maine. *Can. J. Fish. Aquat. Sci.* 74 (11), 1781–1793. <https://doi.org/10.1139/cjfas-2016-0137>.
- Charsley, A.R., Crow, S.K., David, B.O., Smith, J., 2021. Standardised trends of elver abundance in the Waikato. Retrieved from (<https://www.mpi.govt.nz/dmsd/document/47767-FAR-202154-Standardised-trends-of-elver-abundance-in-the-Waikato>).
- A.R. Charsley N. Sibanda S. Hoyle S. Crow. in press. Comparing the performance of three common species distribution modelling frameworks for freshwater environments through application to eel species in New Zealand Canadian Journal of Fisheries and Aquatic Sciences. doi: 10.1139/cjfas-2022-0212.
- Cressie, N., Frey, J., Harch, B., Smith, M., 2006. Spatial prediction on a river network. *J. Agric., Biol., Environ. Stat.* 11 (2), 127–150. <https://doi.org/10.1198/108571106X110649>.
- Crow, S., 2018. New Zealand Freshwater Fish Database (Version 16) [Occurrence dataset]. Retrieved from (<https://doi.org/10.15468/ms15465iqu>): The National Institute of Water and Atmospheric Research (NIWA).
- Crow, S., Snelder, T., Jellyman, P., Greenwood, M., Booker, D., Dunn, A., 2016. Temporal Trends in the Relative Abundance of New Zealand Freshwater Fishes: Analysis of New Zealand Freshwater Fish Database Records. National Institute of Water & Atmospheric Research Ltd, Christchurch, p. 73.
- Crow, S.K., Booker, D., Sykes, J., Unwin, M., Shankar, U., 2014. Predicting distributions of New Zealand freshwater fishes. NIWA Client Rep. CHC2014-145.
- Crow, S.K., Snelder, T., Jellyman, P., Greenwood, M., Booker, D.J., Dunn, A., 2016. Temporal trends in the relative abundance of New Zealand freshwater fishes: analysis of New Zealand freshwater fish database records. NIWA Client Rep. CHC2016-049 73, 71.
- Davey, A.J.H., Jellyman, D.J., 2005. Sex determination in freshwater eels and management options for manipulation of sex. *Rev. Fish. Biol. Fish.* 15 (1), 37–52. <https://doi.org/10.1007/s11160-005-7431-x>.
- Duffy-Anderson, J.T., Stabeno, P., Andrews III, A.G., Ciccioli, K., Deary, A., Farley, E., Fugate, C., Harpold, C., Heintz, R., Kimmel, D., 2019. Responses of the northern Bering Sea and southeastern Bering Sea pelagic ecosystems following record-breaking low winter sea ice. *Geophys. Res. Lett.* 46 (16), 9833–9842. <https://doi.org/10.1029/2019GL083396>.
- Durif, C.M.F., Stockhausen, H.H., Skiftesvik, A.B., Cresci, A., Nyqvist, D., Bowman, H.I., 2022. A unifying hypothesis for the spawning migrations of temperate anguillid eels. *Fish. Fish.* 23 (2), 358–375. <https://doi.org/10.1111/faf.12621>.
- Geffroy, B., Bardonnet, A., 2016. Sex differentiation and sex determination in eels: consequences for management. *Fish. Fish.* 17 (2), 375–398. <https://doi.org/10.1111/faf.12113>.
- Glova, G.J., Jellyman, D.J., 2000. Size-related differences in diel activity of two species of juvenile eel (*Anguilla*) in a laboratory stream. *Ecol. Freshw. Fish.* 9 (4), 210–218. <https://doi.org/10.1111/j.1600-0633.2000.eff090403.x>.
- Glova, G.J., Jellyman, D.J., Bonnett, M.L., 2001. Spatiotemporal variation in the distribution of eel (*Anguilla* spp.) populations in three New Zealand lowland streams. *Ecol. Freshw. Fish.* 10 (3), 147–153. <https://doi.org/10.1034/j.1600-0633.2001.100304.x>.
- Graynoth, E., Booker, D., 2009. Biomass of longfin eels in medium to large rivers. *N. Z. Fish. Assess. Rep.* 44, 24.
- Graynoth, E., Niven, K., 2004. Habitat for female longfinned eels in the West Coast and Southland, New Zealand. Science for Conservation 238, 33 pp. Retrieved from (<https://www.doc.govt.nz/documents/science-and-technical/sfc238.pdf>).
- Graynoth, E., Jellyman, D.J., Bonnett, M., 2008. Spawning escapement of female longfin eels. *N. Z. Fish. Assess. Rep.* 2008/7. Retrieved from ([https://fs.fish.govt.nz/Doc/10549/2008%20FARs/08\\_07\\_FAR.pdf.aspx](https://fs.fish.govt.nz/Doc/10549/2008%20FARs/08_07_FAR.pdf.aspx)).
- Grüss, A., Thorson, J.T., 2019. Developing spatio-temporal models using multiple data types for evaluating population trends and habitat usage. *ICES J. Mar. Sci.* 76 (6), 1748–1761. <https://doi.org/10.1093/icesjms/fsz075>.
- Grüss, A., Thorson, J.T., Sagarase, S.R., Babcock, E.A., Karinauskas, M., Walter III, J.F., Drexler, M., 2017. Ontogenetic spatial distributions of red grouper (*Epinephelus morio*) and gag grouper (*Mycteroperca microlepis*) in the US Gulf of Mexico. *Fish. Res.* 193, 129–142. <https://doi.org/10.1016/j.fishres.2017.04.006>.
- Grüss, A., Biggs, C.R., Heyman, W.D., Erismann, B., 2019. Protecting juveniles, spawners or both? A practical statistical modelling approach for the design of marine protected areas. *J. Appl. Ecol.* 56 (10), 2328–2339. <https://doi.org/10.1111/1365-2664.13468>.
- Grüss, A., Walter III, J.F., Babcock, E.A., Forrestal, F.C., Thorson, J.T., Lauretta, M.V., Schirripa, M.J., 2019. Evaluation of the impacts of different treatments of spatio-temporal variation in catch-per-unit-effort standardization models. *Fish. Res.* 213, 75–93. <https://doi.org/10.1016/j.fishres.2019.01.008>.
- Grüss, A., Gao, J., Thorson, J.T., Rooper, C.N., Thompson, G., Boldt, J.L., Lauth, R., 2020. Estimating synchronous changes in condition and density in eastern Bering Sea fishes. *Mar. Ecol. Prog. Ser.* 635, 169–185. <https://doi.org/10.3354/meps13213>.
- Grüss, A., Rose, K.A., Justić, D., Wang, L., 2020. Making the most of available monitoring data: a grid-summarization method to allow for the combined use of monitoring data collected at random and fixed sampling stations. *Fish. Res.* 229, 105623. <https://doi.org/10.1016/j.fishres.2020.105623>.
- Grüss, A., Pirtle, J.L., Thorson, J.T., Lindeberg, M.R., Neff, A.D., Lewis, S.G., Essington, T.E., 2021. Modeling nearshore fish habitats using Alaska as a regional case study. *Fish. Res.* 238, 105905. <https://doi.org/10.1016/j.fishres.2021.105905>.
- Grüss, A., Thorson, J.T., Stawitz, C.C., Reum, J.C., Rohan, S.K., Barnes, C.L., 2021. Synthesis of interannual variability in spatial demographic processes supports the strong influence of cold-pool extent on eastern Bering Sea walleye pollock (*Gadus chalcogrammus*). *Prog. Oceanogr.* 194 (102569) <https://doi.org/10.1016/j.pocean.2021.102569>.
- Han, Q., Grüss, A., Shan, X., Jin, X., Thorson, J.T., 2021. Understanding patterns of distribution shifts and range expansion/contraction for small yellow croaker (*Larimichthys polyactis*) in the Yellow Sea. *Fish. Oceanogr.* 30 (1), 69–84. <https://doi.org/10.1111/fog.12503>.
- Haro, A., Dekker, W., Bentley, N., 2015. 2013 Independent review of the information available for monitoring trends and assessing the status of New Zealand freshwater eels (2015/2). Retrieved from ([https://fs.fish.govt.nz/Doc/23945/FSR\\_2015\\_02\\_201\\_3\\_Eel\\_Review.pdf.aspx](https://fs.fish.govt.nz/Doc/23945/FSR_2015_02_201_3_Eel_Review.pdf.aspx)).
- Hartig, F., 2020. DHARMA: Residual Diagnostics for Hierarchical (Multi-Level / Mixed) Regression Models: (<https://CRAN.R-project.org/package=DHARMA>).
- Harville, D.A., 1974. Bayesian inference for variance components using only error contrasts. *Biometrika* 61 (2), 383–385. <https://doi.org/10.1093/biomet/61.2.383>.

- Hocking, D.J., Thorson, J.T., O'Neil, K., Letcher, B.H., 2018. A geostatistical state-space model of animal densities for stream networks. *Ecol. Appl.* 28 (7), 1782–1796. <https://doi.org/10.1002/eaap.1767>.
- Hoyle, S.D., 2016. Feasibility of longfin eel stock assessment. *N. Z. Fish. Assess. Rep.* 29, 27.
- Hoyle, S.D., Jellyman, D.J., 2002. Longfin eels need reserves: modelling the effects of commercial harvest on stocks of New Zealand eels. *Mar. Freshw. Res.* 53 (5), 887–895. <https://doi.org/10.1071/MF00020>.
- Isaak, D.J., Peterson, E.E., Ver Hoef, J.M., Wenger, S.J., Falke, J.A., Torgersen, C.E., Sowder, C., Steel, E.A., Fortin, M.J., Jordan, C.E., 2014. Applications of spatial statistical network models to stream data. *Wiley Interdiscip. Rev. Water* 1 (3), 277–294. <https://doi.org/10.1002/wat2.1023>.
- Isaak, D.J., Ver Hoef, J.M., Peterson, E.E., Horan, D.L., Nagel, D.E., 2016. Scalable population estimates using spatial-stream-network (SSN) models, fish density surveys, and national geospatial database frameworks for streams. *Can. J. Fish. Aquat. Sci.* 74 (2), 147–156. <https://doi.org/10.1139/cjfas-2016-0247>.
- Jacoby, D., Casselman, J., DeLucia, M., Gollcock, M., 2017. *Anguilla rostrata* (amended version of 2014 assessment). IUCN Red. List Threat. Species 2017.
- Jellyman, D.J., Chisnall, B.L., Bonnett, M.L., Sykes, J.R.E., 1999. Seasonal arrival patterns of juvenile freshwater eels (*Anguilla* spp.) in New Zealand. *N. Z. J. Mar. Freshw. Res.* 33 (2), 249–261. <https://doi.org/10.1080/00288330.1999.9516874>.
- Jellyman, D.J., Chisnall, B.L., Sykes, J.R.E., Bonnett, M.L., 2002. Variability in spatial and temporal abundance of glass eels (*Anguilla* spp.) in New Zealand waterways. *N. Z. J. Mar. Freshw. Res.* 36 (3), 511–517. <https://doi.org/10.1080/00288330.2002.9517106>.
- Jellyman, D.J., 1997. Variability in growth rates of freshwater eels (*Anguilla* spp.) in New Zealand. *Ecol. Freshw. Fish.* 6 (2), 108–115. <https://doi.org/10.1111/j.1600-0633.1997.tb00151.x>.
- Jellyman, D.J., Bonnett, M.L., Sykes, J.R.E., Johnstone, P., 2003. Contrasting use of daytime habitat by two species of freshwater eel *Anguilla* spp. in New Zealand rivers. In American Fisheries Society Symposium. American Fisheries Society, pp. 63–78.
- Jellyman, D., Graynoth, E., 2005. The use of fyke nets as a quantitative capture technique for freshwater eels (*Anguilla* spp.) in rivers. *Fish. Manag. Ecol.* 12 (4), 237–247.
- Johnson, K.F., Councill, E., Thorson, J.T., Brooks, E., Methot, R.D., Punt, A.E., 2016. Can autocorrelated recruitment be estimated using integrated assessment models and how does it affect population forecasts. *Fish. Res.* 183, 222–232. <https://doi.org/10.1016/j.fishres.2016.06.004>.
- Jowett, I.G., Richardson, J., 1995. Habitat preferences of common, riverine New Zealand native fishes and implications for flow management. *N. Z. J. Mar. Freshw. Res.* 29 (1), 13–23. <https://doi.org/10.1080/00288330.1995.9516635>.
- Jowett, I.G., Richardson, J., 1996. Distribution and abundance of freshwater fish in New Zealand rivers. *N. Z. J. Mar. Freshw. Res.* 30 (2), 239–255. <https://doi.org/10.1080/00288330.1996.9516712>.
- Joy, M., David, B., Lake, M., 2013. New Zealand Freshwater Fish Sampling Protocols. Massey University, Palmerston North, New Zealand.
- Joy, M.K., Foote, K.J., McNie, P., Piria, M., 2018. Decline in New Zealand's freshwater fish fauna: effect of land use. *Mar. Freshw. Res.* 70 (1), 114–124. <https://doi.org/10.1071/MF18028>.
- Kai, M., Thorson, J.T., Piner, K.R., Maunder, M.N., 2017. Spatiotemporal variation in size-structured populations using fishery data: an application to shortfin mako (*Isurus oxyrinchus*) in the Pacific Ocean. *Can. J. Fish. Aquat. Sci.* 74 (11), 1765–1780. <https://doi.org/10.1139/cjfas-2016-0327>.
- Kass, R.E., Steffey, D., 1989. Approximate Bayesian inference in conditionally independent hierarchical models (parametric empirical Bayes models. *J. Am. Stat. Assoc.* 84 (407), 717–726. <https://doi.org/10.1080/01621459.1989.10478825>.
- Kristensen, K., Nielsen, A., Berg, C.W., Skaug, H., Bell, B., 2015. TMB: automatic differentiation and Laplace approximation. *J. Stat. Softw.* 70, 1–20. <https://arxiv.org/g/ct?url=https%3A%2F%2Fdx.doi.org%2F10.18637%2Fjss.v070.i05&v=170d42e1>.
- International Council for the Exploration of the Sea (ICES), 2018. Joint EIFAAC/ICES/GFCM Working Group on Eels (WGEEEL), 5–12 September 2018, Gdańsk, Poland. ICES CM 2018/ACOM:15. 152 pp. doi: 10.17895/ices.pub.20418840.v2.
- Leathwick, J.R., Julian, K., Elith, J., Rowe, D., 2008. Predicting the distributions of freshwater fish species for all New Zealand's rivers and streams (NIWA Client Report, HAM2008–005). Retrieved from [https://niwa.co.nz/sites/niwa.co.nz/files/29\\_nationalfishpredictionmaps.pdf](https://niwa.co.nz/sites/niwa.co.nz/files/29_nationalfishpredictionmaps.pdf).
- Li, J., Hatton-Ellis, T.W., Lawson Handley, L.J., Kimbell, H.S., Benucci, M., Peirson, G., Häfling, B., 2019. Ground-truthing of a fish-based environmental DNA metabarcoding method for assessing the quality of lakes. *J. Appl. Ecol.* 56 (5), 1232–1244.
- Lindgren, F., Rue, H., Lindström, J., 2011. An explicit link between Gaussian fields and Gaussian Markov random fields: the stochastic partial differential equation approach. *J. R. Stat. Soc. Ser. B Stat. Methodol.* 73 (4), 423–498.
- Lo, N.C.-h., Jacobson, L.D., Squire, J.L., 1992. Indices of relative abundance from fish spotter data based on delta-lognormal models. *Can. J. Fish. Aquat. Sci.* 49 (12), 2515–2526. <https://doi.org/10.1139/f92-278>.
- Malcolm, I.A., Millidine, K.J., Jackson, F.L., Glover, R.S., Fryer, R.J., 2020. The national electrofishing programme for Scotland (NEPS) 2019. Retrieved from <https://data.marine.gov.scot/sites/default/files//SMFS%201109.pdf>.
- McDowall, R.M., 1990. New Zealand Freshwater Fishes: A Natural History and Guide. Heinemann Reed, Auckland, New Zealand.
- McDowall, R.M., Taylor, M.J., 2000. Environmental indicators of habitat quality in a migratory freshwater fish fauna. *Environ. Manag.* 25 (4), 357–374. <https://doi.org/10.1007/s002679910028>.
- Ohlberger, J., Scheuerell, M.D., Schindler, D.E., 2016. Population coherence and environmental impacts across spatial scales: a case study of Chinook salmon. *Ecosphere* 7 (4), e01333. <https://doi.org/10.1002/ecs2.1333>.
- Peterson, E.E., Ver Hoef, J.M., Isaak, D.J., Falke, J.A., Fortin, M.J., Jordan, C.E., McNyset, K., Monestiez, P., Ruesch, A.S., Sengupta, A., 2013. Modelling dendritic ecological networks in space: an integrated network perspective. *Ecol. Lett.* 16 (5), 707–719. <https://doi.org/10.1111/ele.12084>.
- Pike, C., Crook, V., Gollcock, M., 2019. *Anguilla dieffenbachii* (errata version published in 2019). In The IUCN Red List of Threatened Species 2019: eT197276A154802213.
- R Core Team, 2020. R: A Language and Environment for Statistical Computing. R Foundation for Statistical Computing, Vienna, Austria. (<https://www.R-project.org/>).
- Shortland, T., Tipene-Thomas, J., 2019. Inventory of iwi and hapu eel research. Retrieved from <https://fs.fish.govt.nz/Doc/24686/FAR-2019-15-Inventory-of-iwi-and-hapu-eel-research.pdf.ashx>.
- Snelder, T.H., Biggs, B.J.F., 2002. Multiscale river environment classification for water resources management. *J. Am. Water Resour. Assoc.* 38 (5), 1225–1239. <https://doi.org/10.1111/j.1752-1688.2002.tb04344.x>.
- Snelder, T.H., Cattanéo, F., Suren, A.M., Biggs, B.J.F., 2004. Is the River environment classification an improved landscape-scale classification of rivers? *J. North Am. Benthol. Soc.* 23 (3), 580–598. [https://doi.org/10.1899/0887-3593\(2004\)023%3C0580:ITRECA%3E2.0.CO;2](https://doi.org/10.1899/0887-3593(2004)023%3C0580:ITRECA%3E2.0.CO;2).
- Stefánsson, G., 1996. Analysis of groundfish survey abundance data: combining the GLM and delta approaches. *ICES J. Mar. Sci.* 53 (3), 577–588. <https://doi.org/10.1006/jmsc.1996.0079>.
- Stow, C.A., Jolliff, J., McGillicuddy, D.J.J., Doney, S.C., Allen, J.I., Friedrichs, M.A., Rose, K.A., Wallhead, P., 2009. Skill assessment for coupled biological/physical models of marine systems. *J. Mar. Syst.* 76 (1–2), 4–15. <https://doi.org/10.1016/j.jmarsys.2008.03.011>.
- Tanaka, E., 2014. Stock assessment of Japanese eels using Japanese abundance indices. *Fish. Sci.* 80 (6), 1129–1144. <https://doi.org/10.1007/s12562-014-0807-x>.
- Thorson, J.T., 2019c. VAST model structure and user interface. <https://github.com/James-Thorson-NOAA/VAST>.
- Thorson, J.T., 2015. Spatio-temporal variation in fish condition is not consistently explained by density, temperature, or season for California current groundfishes. *Mar. Ecol. Prog. Ser.* 526, 101–112. <https://doi.org/10.3354/meps11204>.
- Thorson, J.T., 2018. Three problems with the conventional delta-model for biomass sampling data, and a computationally efficient alternative. *Can. J. Fish. Aquat. Sci.* 75 (9), 1369–1382. <https://doi.org/10.1139/cjfas-2017-0266>.
- Thorson, J.T., 2019. Guidance for decisions using the Vector Autoregressive Spatio-Temporal (VAST) package in stock, ecosystem, habitat and climate assessments. *Fish. Res.* 210, 143–161. <https://doi.org/10.1016/j.fishres.2018.10.013>.
- Thorson, J.T., 2019. Forecast skill for predicting distribution shifts: a retrospective experiment for marine fishes in the Eastern Bering Sea. *Fish. Fish.* 20 (1), 159–173. <https://doi.org/10.1111/faf.12330>.
- Thorson, J.T., Barnett, L.A.K., 2017. Comparing estimates of abundance trends and distribution shifts using single- and multispecies models of fishes and biogenic habitat. *ICES J. Mar. Sci.* 74 (5), 1311–1321. <https://doi.org/10.1093/icesjms/fsw193>.
- Thorson, J.T., Haltuch, M.A., 2018. Spatiotemporal analysis of compositional data: increased precision and improved workflow using model-based inputs to stock assessment. *Can. J. Fish. Aquat. Sci.* 76 (3), 401–414. <https://doi.org/10.1139/cjfas-2018-0015>.
- Thorson, J.T., Kristensen, K., 2016. Implementing a generic method for bias correction in statistical models using random effects, with spatial and population dynamics examples. *Fish. Res.* 175, 66–74. <https://doi.org/10.1016/j.fishres.2015.11.016>.
- Thorson, J.T., Shelton, A.O., Ward, E.J., Skaug, H.J., 2015. Geostatistical delta-generalized linear mixed models improve precision for estimated abundance indices for West Coast groundfishes. *ICES J. Mar. Sci.* 72 (5), 1297–1310. <https://doi.org/10.1093/icesjms/fsu243>.
- Thorson, J.T., Scheuerell, M.D., Shelton, A.O., See, K.E., Skaug, H.J., Kristensen, K., 2015. Spatial factor analysis: a new tool for estimating joint species distributions and correlations in species range. *Methods Ecol. Evol.* 6 (6), 627–637. <https://doi.org/10.1111/2041-210x.12359>.
- Thorson, J.T., Rindorf, A., Gao, J., Hanselman, D.H., Winker, H., 2016. Density-dependent changes in effective area occupied for sea-bottom-associated marine fishes. *Proc. R. Soc. B Biol. Sci.* 283 (1840), 20161853. <https://doi.org/10.1098/rspb.2016.1853>.
- Thorson, J.T., Adams, G., Holsman, K., 2019. Spatio-temporal models of intermediate complexity for ecosystem assessments: a new tool for spatial fisheries management. *Fish. Fish.* 20 (6), 1083–1099. <https://doi.org/10.1111/faf.12398>.
- Ver Hoef, J., Peterson, E., Clifford, D., Shah, R., 2014. SSN: An R package for spatial statistical modeling on stream networks. *J. Stat. Softw.* 56 (1), 1–45. <https://doi.org/10.18637/jss.v056.i03>.
- Ver Hoef, J.M., Peterson, E.E., 2010. A moving average approach for spatial statistical models of stream networks. *J. Am. Stat. Assoc.* 105 (489), 6–18. <https://doi.org/10.1198/jasa.2009.ap08248>.
- Ver Hoef, J.M., Peterson, E.E., Theobald, D., 2006. Spatial statistical models that use flow and stream distance. *Environ. Ecol. Stat.* 13 (4), 449–464. <https://doi.org/10.1007/s10651-006-0022-8>.
- Ver Hoef, J.M., Peterson, E.E., Isaak, D.J., 2019. Spatial statistical models for stream networks. In *Handbook of Environmental and Ecological Statistics*. Chapman and Hall/CRC, pp. 421–444.
- Weldon, L., O'Leary, C., Steer, M., Newton, L., Macdonald, H., Sargeant, S.L., 2020. A comparison of European eel *Anguilla anguilla* eDNA concentrations to fyke net catches in five Irish lakes. *Environ. DNA* 2 (4), 587–600. <https://doi.org/10.1002/edn3.91>.